Abstract

Periodic Behavior of Stator Upstream Cavity Flow in a Multistage Axial Compressor

KEIBYEONG LEE
School of Mechanical and Aerospace Engineering
Graduate School
Seoul National University

To investigate upstream cavity flow to main flow interaction, three dimensional ensemble averaged velocity measurement has been conducted inside the shrouded stator upstream cavity and adjacent main passage. To obtain three dimensional flow field, one dimensional hotwire measurement for three different yaw angle has been conducted. Periodic unsteady radial jet is the main factor which makes difference between phase locked ensemble averaged data and steady data. Periodic unsteady radial jet moves with the same speed of the rotor wake with periodic generation and dissipation. At the interface of cavity flow and main passage flow which is 0% of span, negative radial velocity(ingress) is dominant. However when periodic unsteady radial jet approaches, positive radial directional(egress) velocity becomes dominant inside of the cavity. Also time averaged data of this study coincide with steady simulation of previous research. Flow inside of cavity has certain partial circular structure just like previous research for the most of the time, however as periodic radial jet approaches, the

structure destroyed and negative radial directional velocity(egress) become dominant. Moreover periodic unsteady radial jet exist upstream and downstream of cavity. Also periodic unsteady radial jet propagates to the next stage, it should be considered at the designing step of a compressor.

Keyword : Axial Compressor, Periodic measurement, Shroud, Cavity, Leakage
Student Number : 2015-20739

Table of Contents

List of Figures

List of Tables

Nomenclature

ϕ_d	Design flow coefficient
$Re_{c,\theta}$	Reynolds number at the stator main passage
ψ	Pressure coefficient
θ_0	Wire angle
θ_p	Pitch angle
θ_y	Yaw angle
E	Voltage
U	Velocity of target flow
α	Angle between flow and wire
U_t	Velocity at rotor tip
U_r	Radial velocity
U_x	Axial velocity
r	Radial direction
θ	Tangential direction
x	Axial direction
Ω	Angular velocity
r	Radius of rotor
C_p	Pressure coefficient
A	Area

Chapter 1. Introduction

1.1. Research Background

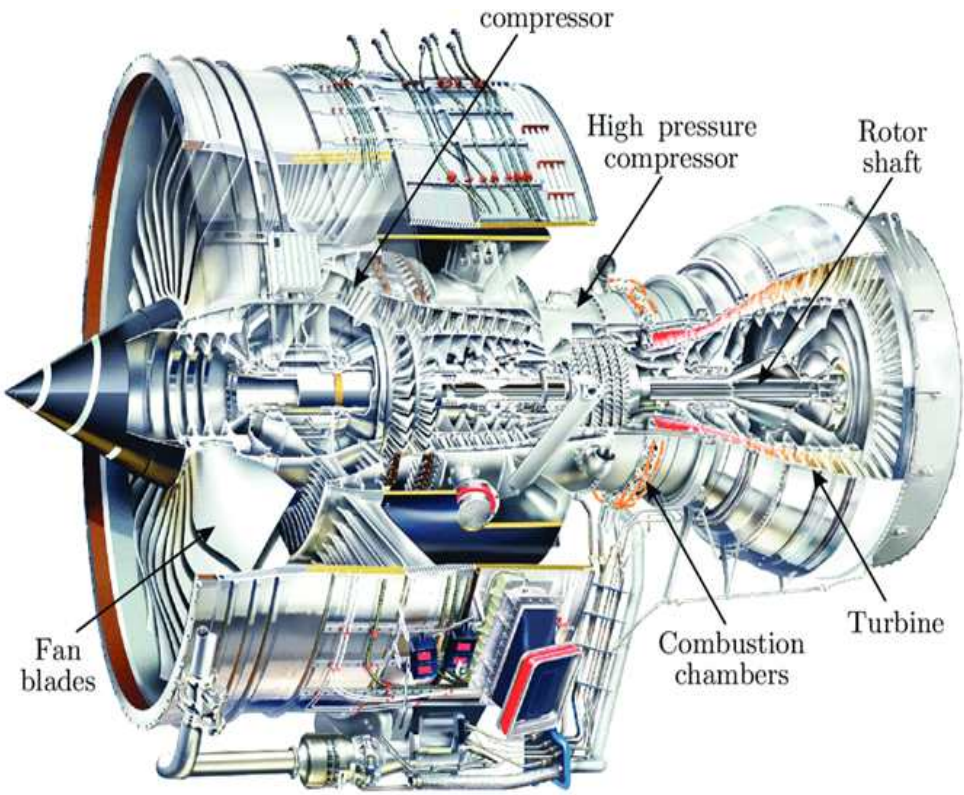

Figure 1.1. Jet engine turbofan: Rolls Royce Trent 900

Jet engine is consisted of compressor, combustor and turbine. In aerospace application, axial compressor which main flow direction and the axis of compressor have same direction is mainly used. Axial compressor has two parts. Ones is rotational part which is called as rotor and the other is stationary part which is called as stator. Rotors give energy to the main fluid and stator mainly changing flow direction to make static pressure rise of a compressor. Because rotor rotates with respect to stator, there is inevitable gap between rotor

and stator and there is two types of stator gab. One is cantilevered type of stator gap(figure 1.2.) which has simple sap between stator and hub shaft and the other(figure 1.3.) is shrouded type which has band at the hub side of stator and labyrinth seal①. For the case of shrouded type, the band at the hub side dedicate to high mechanical integrity so that it is more preferred. Because stator downstream has high static pressure, flow leaks through the gaps form downstream of stator to upstream of stator. This leakage flow deteriorate compressor performance.

In the case of shrouded type, even though leakage flow through cavity is major source of loss, knowledge about how the cavity flow and main flow interact is very limited.

① Wellborn & Okiishi, 1996

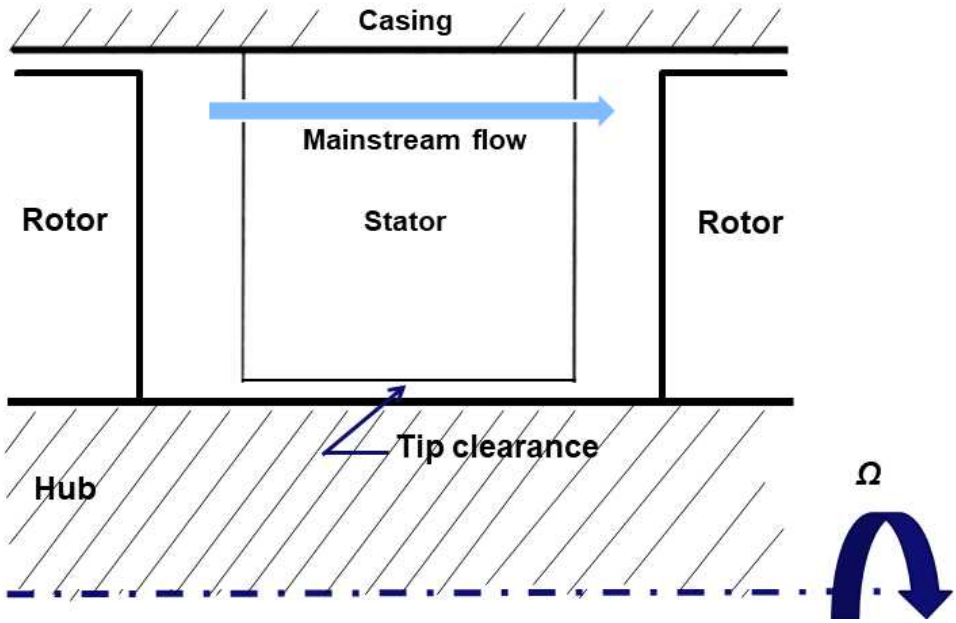

Figure 1.2. Cantilevered type stator

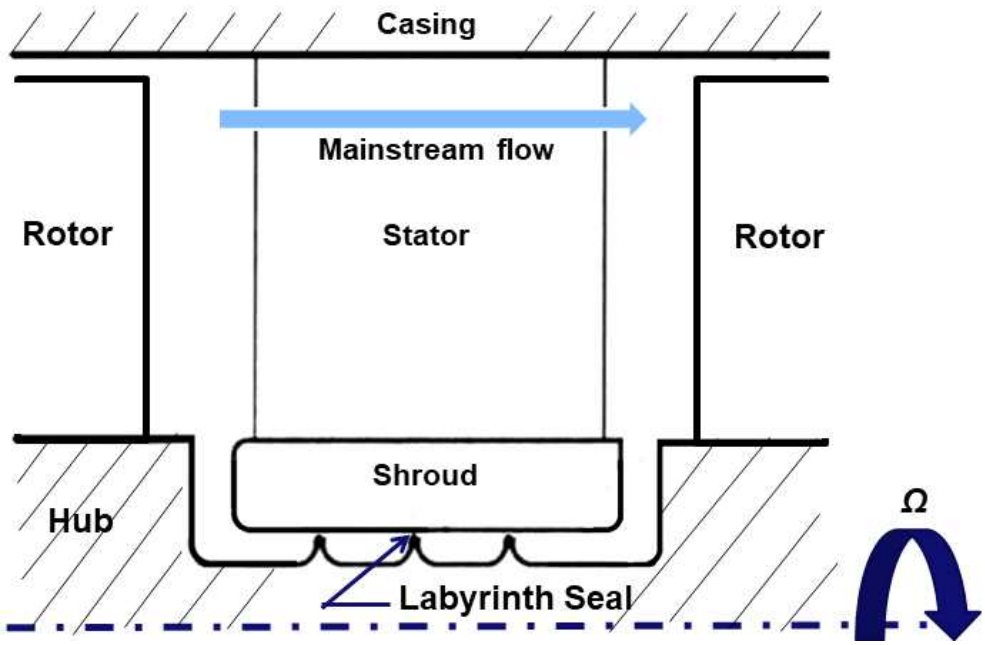

Figure 1.3. Shrouded type stator

1.2. Previous Research

There was a lot of study about stator hub leakage flow effect in steady condition. Yoon et al.[1] simulated different stator hub gap configuration which are shrouded type and cantilever type. They found that reaction, solidity, rotating and stationary part clearance determine loss. Also they concluded for high reaction blade shrouded type is generally better in efficiency because of low loss coefficient. Wellborn and Okishi[2] performed experiment and conducted simulation in 4 stage axial compressor. They measured detailed flow structure inside stator cavity and linked tangential velocity of stator cavity leakage flow to overall loss. They correlated that increase of seal gap in 1 percent of blade span detriment 3 percent pressure rise and 1 percent efficiency. Also Heidegger et al.[3] linked increase seal gap to recduction of compressor performance in their simulation. Lange et al.[4] performed multistage condition experiment for cantilever and shrouded type stator gap and found that shrouded type has lower efficiency because of hub corner separation on stator suction side.

Recently more and more research focus on unsteady effect. Kato et al. [5] performed unsteady simulation in multistage axial compressor and they insisted importance of unsteady behavior of flow because unsteady wake interacts with leakage flow and generate more loss. Mailach et al. [6] conducted hot film and LDV

measurement to study Stator wake – Rotor tip clearance vortex interaction. they found out Stator wake cause tip clearance vortex fluctuation. Montomoli et al. [7] conducted steady and unsteady simulations of the cantilever stator configuration in multistage condition. Their conclusion was unsteady cases has higher operating range and lower losses than steady cases.

1.3. Research Motivation and Objectives

1n the case of shrouded type, even though leakage flow through cavity is major source of loss and steady flow structure inside of cavity(figure1 1.4.②) was well established, recent unsteady research only has focused on understanding main passage and casing region flow behavior of stator[5, 6, 7]. Still knowledge about how the cavity flow and main flow interact is still unknown.

This study focus on periodic unsteady behavior of stator upstream cavity flow and its interaction with main flow. so the objective of this study is as follows.

1. Conduct three dimensional velocity measurement inside cavity and adjacent main passage at the five different planes to understand periodic behavior of stator upstream cavity flow.

2. Find out how stator upstream cavity flow interact with main flow by focusing on interface of cavity flow and main flow

② Wellborn, 2001

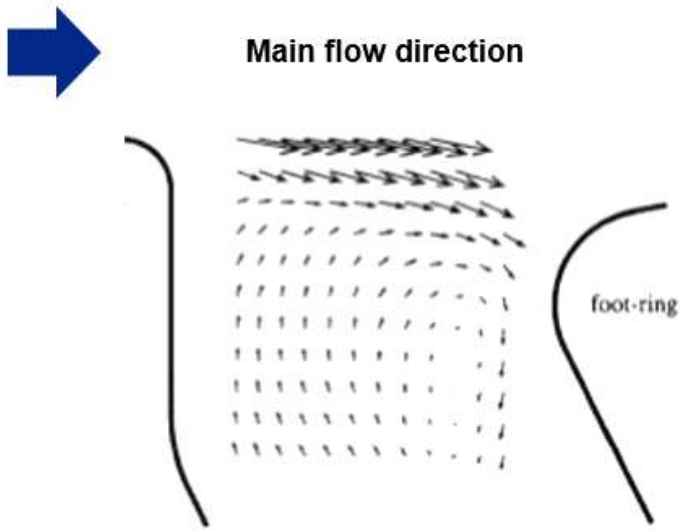

Figure 1.4. Steady measurement of upstrem cavity by Wellborn

Chapter 2. Apparatus

2.1. Seoul National University Compressor(LSRC)

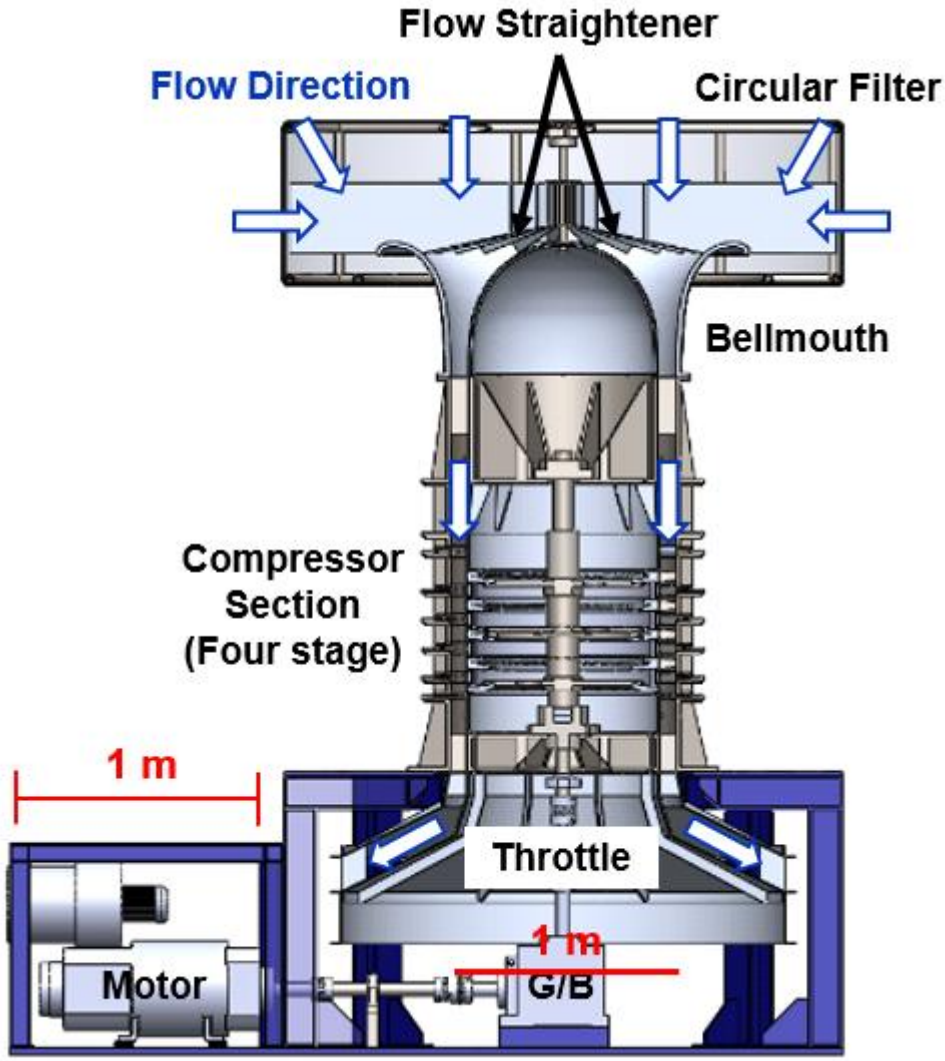

Figure 2.1. Seoul National University Compressor (LSRC)

Figure 2.1 is vertically aligned plane sliced view of the Seoul National University Compressor LSRC(Low Speed Research Compressor) which is the machine by with this study conducted. LSRC is vertically aligned open type axial compressor which flow go

in at the top of the compressor. Above the bellmouth circular filter and flow straightener were installed to prevent dust and tangential direction velocity component. 55kw DC motor and gearbox drives power to the compressor and flow rate is controlled by throttle which is operated by four vertically moving linear actuator. LSRC have four repeating stages and IGV(inlet guide vane).

Table 2.1. shows parameters of LSRC. Its design flow coefficient is 0.365 and rpm is 1000 and $Re_{c,\theta}$ is 195,000. Blade number of IGV, Rotor and Stator are 53, 52, 88 respectively. Tip radious is 500mm and Hub to Tip Ratio which means radial length of hub divided by radial length of tip is 0.85. Actual rotor chord is 56mm and stator chord is 50mm. Tip clearance which means gap between blade tip and casing is 1.4% of span and seal clearance which means gap between shroud to labyrinth seal is 0.9% of span.

Parameter	Value
$\Phi_d (= C_x / U_{tip})$	0.365
# of IGV/Rotor/Stator	53/52/88
Tip Radius(mm)	500
Hub to Tip Ratio	0.85
Rotor Chord(mm)	56
Stator Chord(mm)	50
Tip Clearance	1.4% Span
Seal Clearance	0.9% Span
RPM	1,000
$Re_{c,\theta}$	195,000

Table 2.1. Parameters of LSRC

Figure 2.2. Picture of LSRC

2.2. Compressor Map of LSRC and Experiment Condition

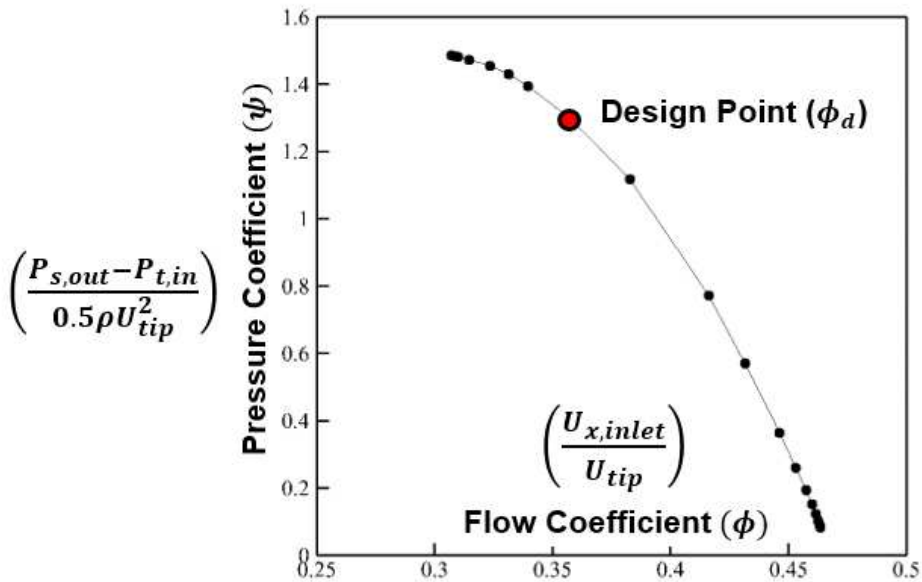

Figure 2.3. Compressor map of LSRC.

Figure 2.3 shows compressor map of LSRC. X axis is flow coefficient defined by $\Phi = \frac{C_x}{U_{tip}}$ and Y axis is pressure coefficient defined by $\Psi = \frac{\Delta P}{0.5\rho U_{tip}^2}$. Design condition is a operating point which has highest efficiency so that condition of the point is normal operating condition. Mass flow rate at the design condition is 5kg/s and this study was conducted at design condition.

Chapter 3. Measurement Planes and Method

3.1. Measurement Planes and Grids

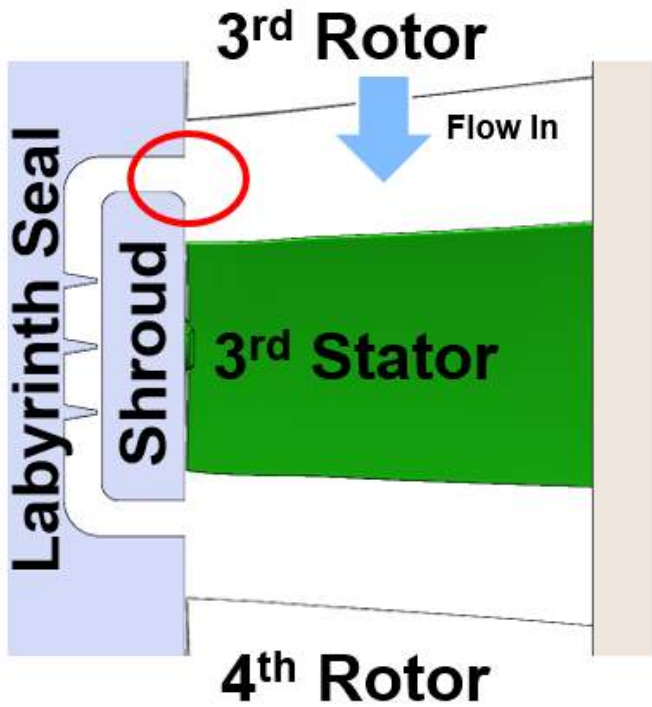

Figure 3.1. Measurement region

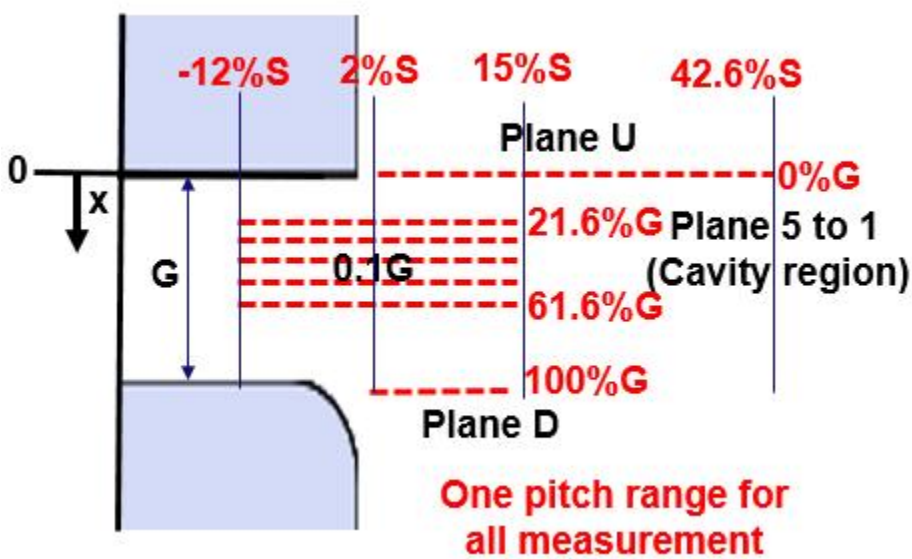

Figure 3.2. Measurement planes

Figure 3.1. represent measurement region which is 3rd upstream cavity and Figure 3.2. represent measurement planes with enlarged view of red circle of figure 3.1. Measurement was conducted at 7 different $r-\theta$ planes which is in and adjacent main passage regain of 3rd stage stator upstream cavity. Five planes spans radially from -12% of span to 15% of span and this planes spans axially from 21.6% of axial cavity gap to 61.6% of axial cavity gap from cavity upstream wall by 10% of axial cavity gap spacing. Plane U which located at the upstream of upstream cavity is spans from 2% of span to 42.6% of span and plane D which located at downstream of upstream cavity spans from 2% of span to 15% of span. All of the planes have one pitch range.

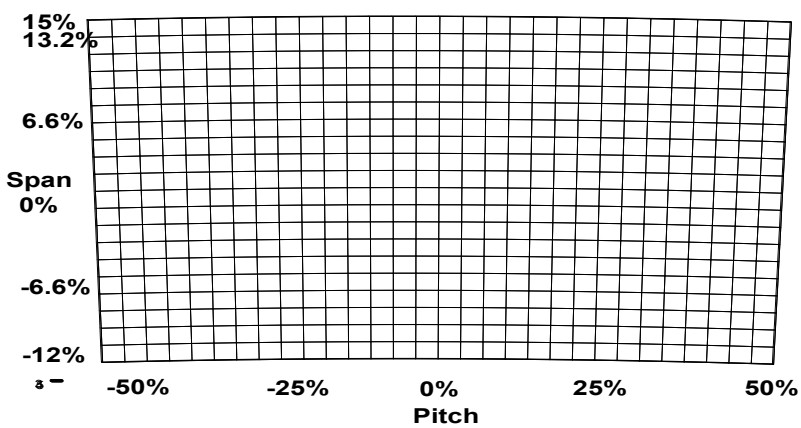

Figure 3.3. Gird of plane 1 to 5

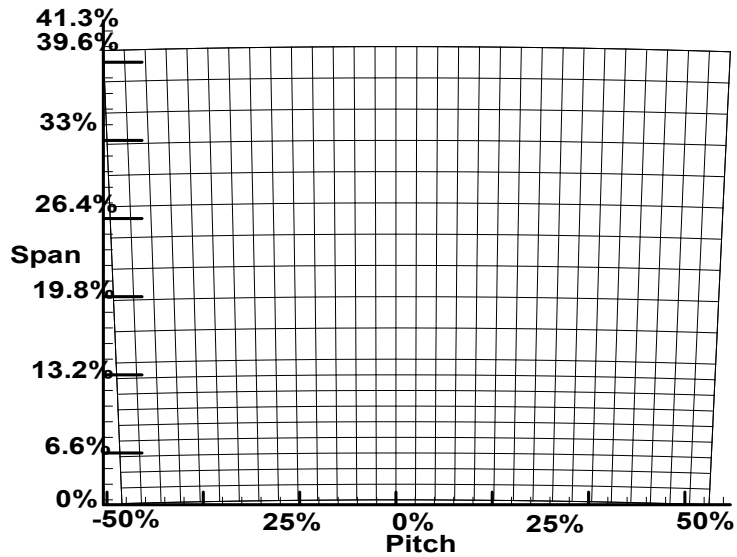

Figure 3.4. Gird of plane U

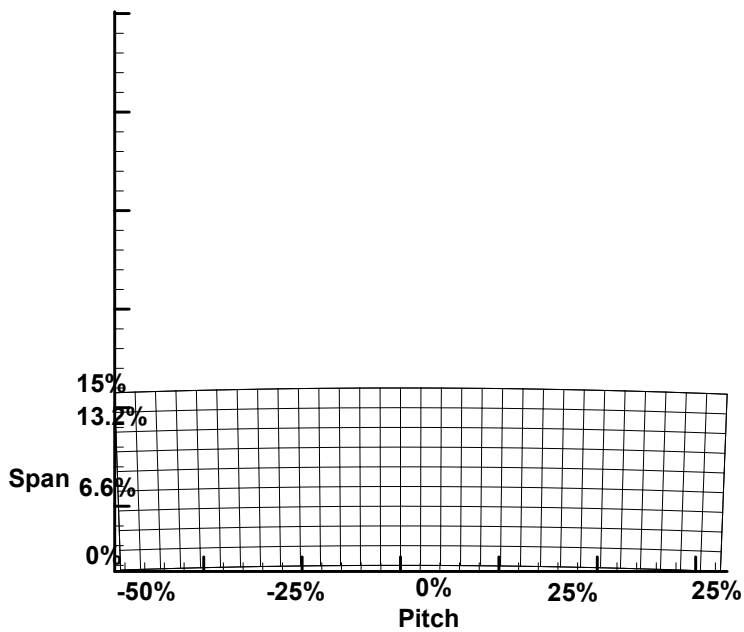

Figure 3.5. Grid of plane D

To investigate flow field inside of the cavity and cavity to mainstream interface, tangentially 31points and radially 21points were assigned to plane 1-5 so that for each cavity region plane total 651points were measured. For the plane U tangentially 31points and radially 20points and for the plane D tangentially 31points and radially 10points were measured. Total number of points were 620 and 310 respectively.

3.2. Measurement Method

3.2.1. Hot Wire Rotating Technique

To measure three dimensional velocity vector, one dimensional 45 degree slanted hot wire was used.

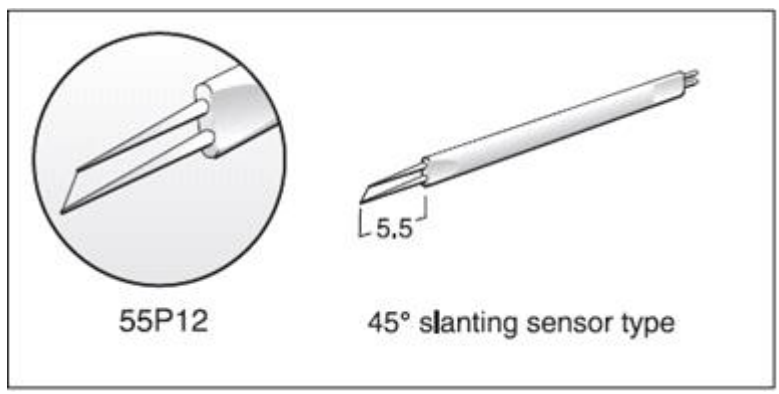

Figure 3.6. One dimensional slanted miniature DANTEC 55P12 hot wire

To get three dimensional velocity component, three measurement with different yaw angle spaced by 40 degree was needed. However hotwire probe cannot be rotated by the speed rotating time that can be neglected, phase locked ensemble average technique with encoder was used.

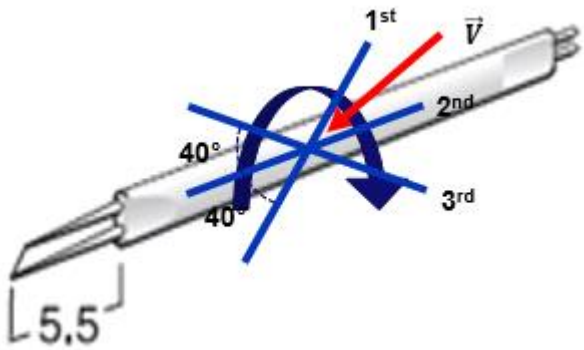

Figure 3.7. One dimensional hot wire rotating technique [8]

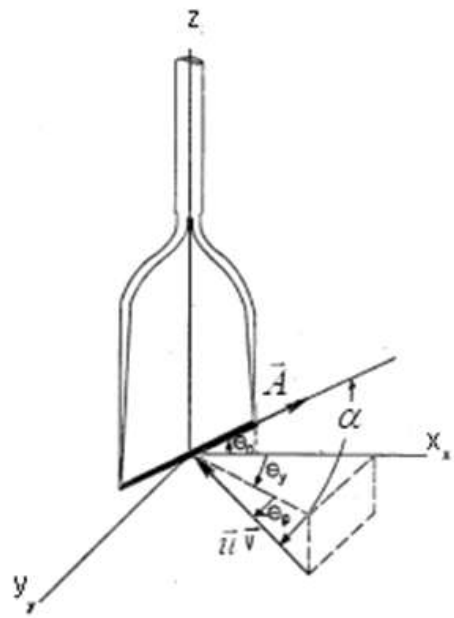

Figure 3.8. Coordination System of on dimensional hot-wire and flow velocity vector[9]

According to dantech streamline users guide, row voltage at three different yaw angle can be converted to effective voltage by which magnitude and direction of the flow can be determined.

First, obtain correlation of effective velocity and Constant Temperature Anemometer(CTA) voltage

$$U_{eff} = a_4E^4 + a_3E^3 + a_2E^2 + a_1E^1 + a_0$$

Second, conduct pitch and yaw response calibration to find out coefficient of equation below[9].

$$(\frac{U_{eff}}{U}) = a_0 + a_1\alpha + a_2\theta_p + a_3U + a_4\alpha\theta_p + a_5\alpha U + a_6\theta_p U + a_7\theta_p^2 + a_8\alpha^2 + a_9\alpha^2$$

Third, with the equation above and below, find out six unknown (α_1, α_2, α_3, U, θ_p, θ_y) by using matlab code 'fslove'. For each yaw angle we can get different two equation

$$\cos\alpha = \cos\theta_0\cos\theta_p\cos\theta_y - \sin\theta_o\sin\theta_p.$$

This method has 6.67% of U 1.52° angle uncertainty.

3.2.2. Traverse System

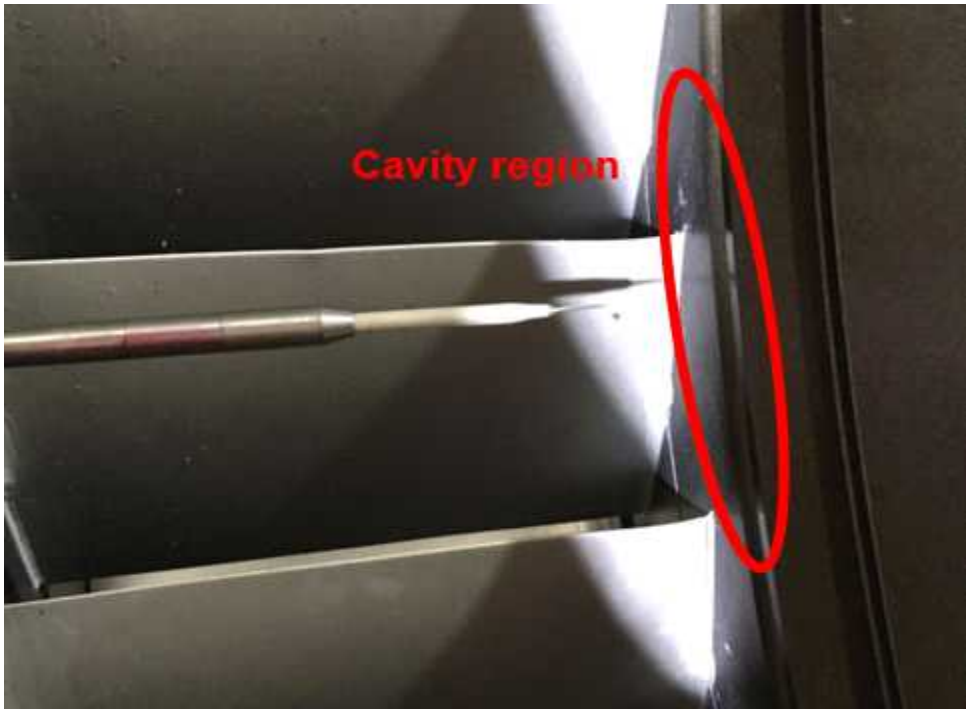

Figure 3.9. Hotwire and cavity position

Figure 3.10. Hotwire position inside of cavity

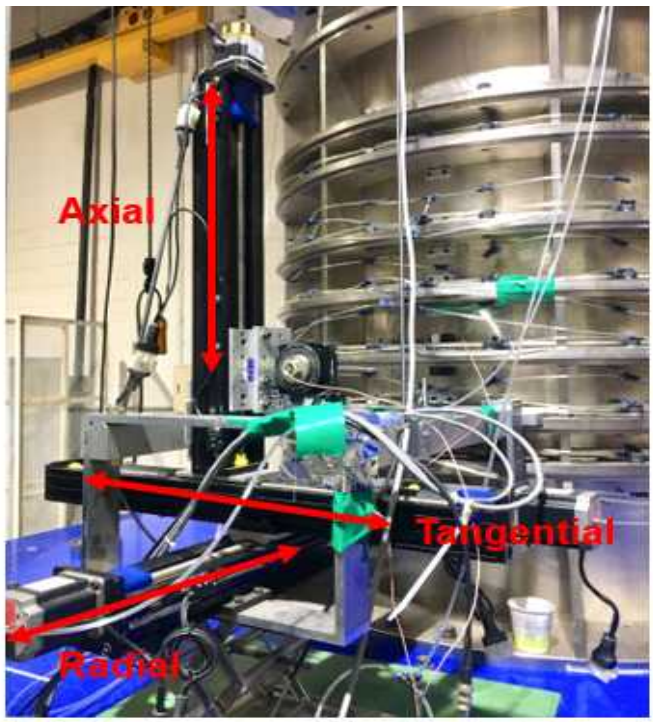

Figure 3.11. Three axis traverse system

Figure 3.6 shows hotwire approaching way with respect to stator blade. Hotwire was inserted from the casing side of compressor by radial traverse. Dimensional axial gap of the stator upstream cavity is only 6mm and axial gap of cavity region planes(plane5 to 1) is only 0.6mm so that very accurate positioning was necessary. To achieve precise positioning, three axis traverse system was introduced. It is combination of three linear traverse and mounted vertically one another.

Chapter 4. Experiment Results and Analysis

4.1. Periodic Unsteady Phenomena

4.1.1. Periodic Unsteady Radial Jet at the Radial Tangential Plane

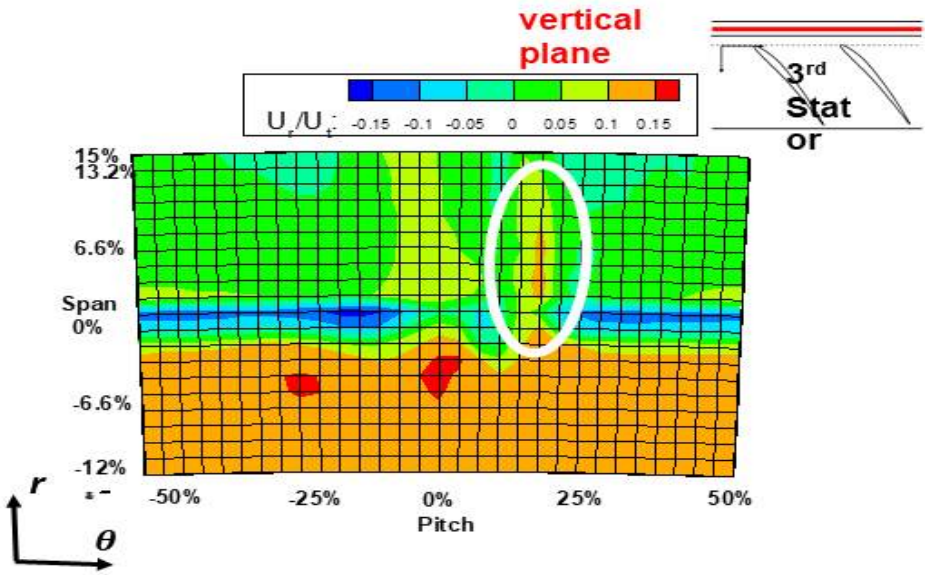

Figure 4.1.1 Radial-Tangential contour of Ur
Timestep 0/30

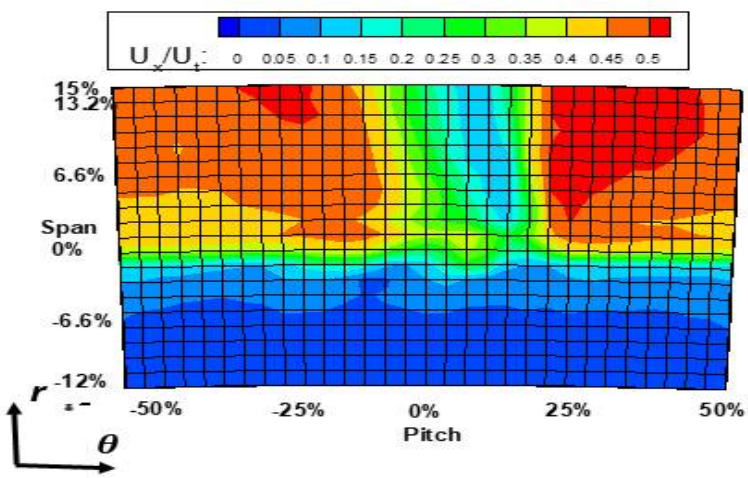

Figure 4.1.2 Radial-Tangential contour of Ux
Timestep 0/30

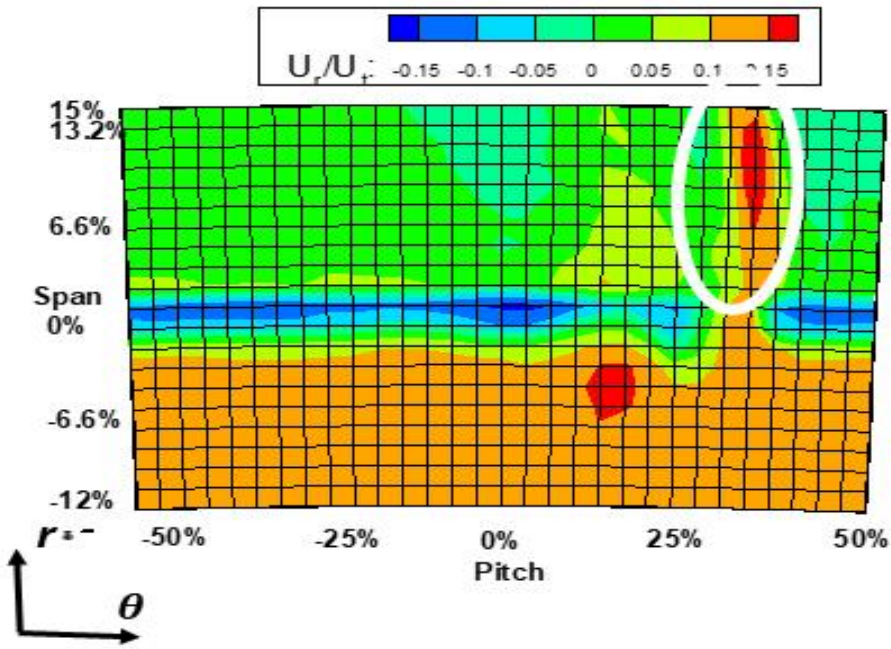

Figure 4.1.3 Radial-Tangential contour of Ur
Timestep 5/30

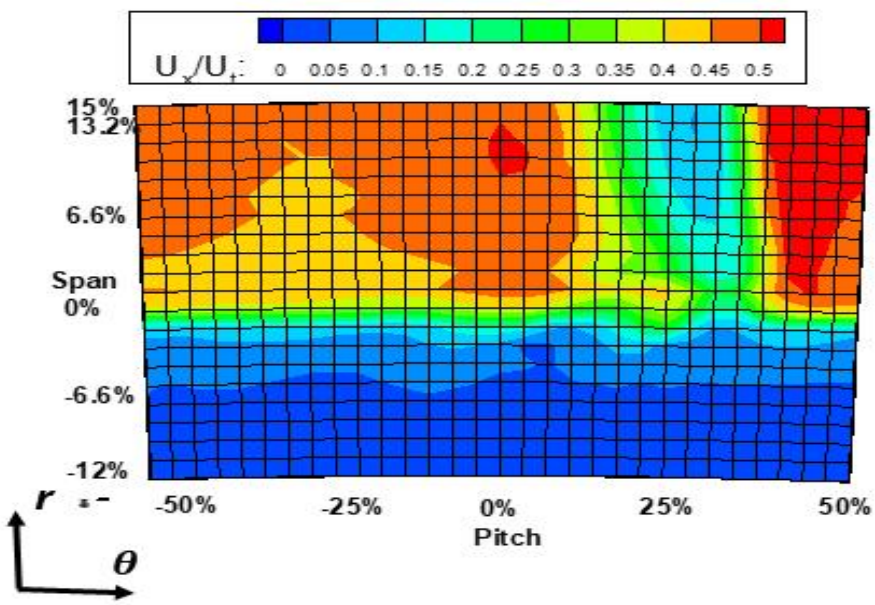

Figure 4.1.4 Radial-Tangential contour of Ux
Timestep 5/30

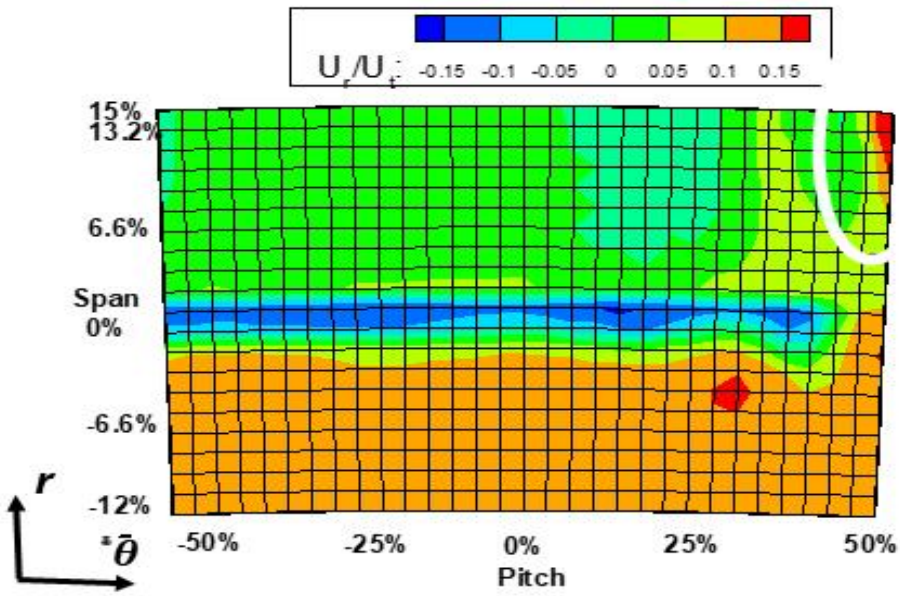

Figure 4.1.5 Radial-Tangential contour of Ur
Timestep 10/30

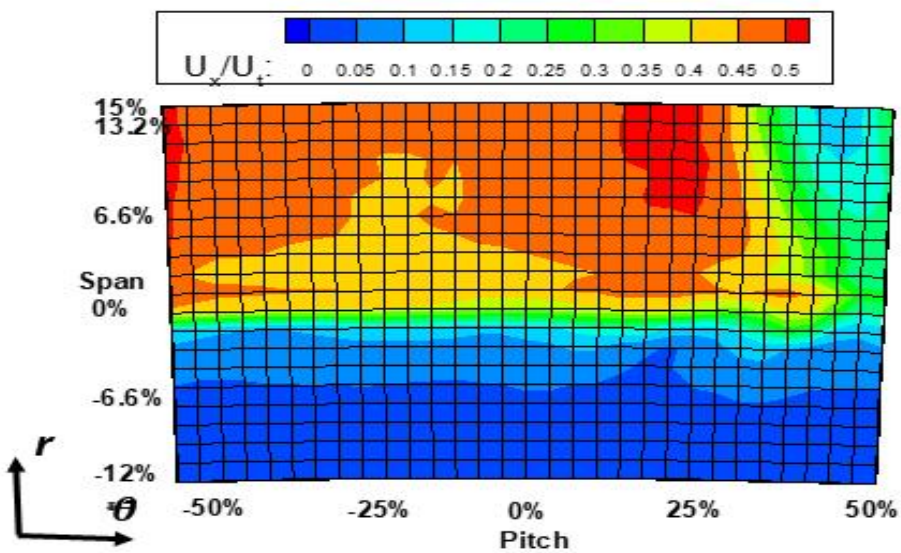

Figure 4.1.6 Radial-Tangential contour of Ux
Timestep 10/30

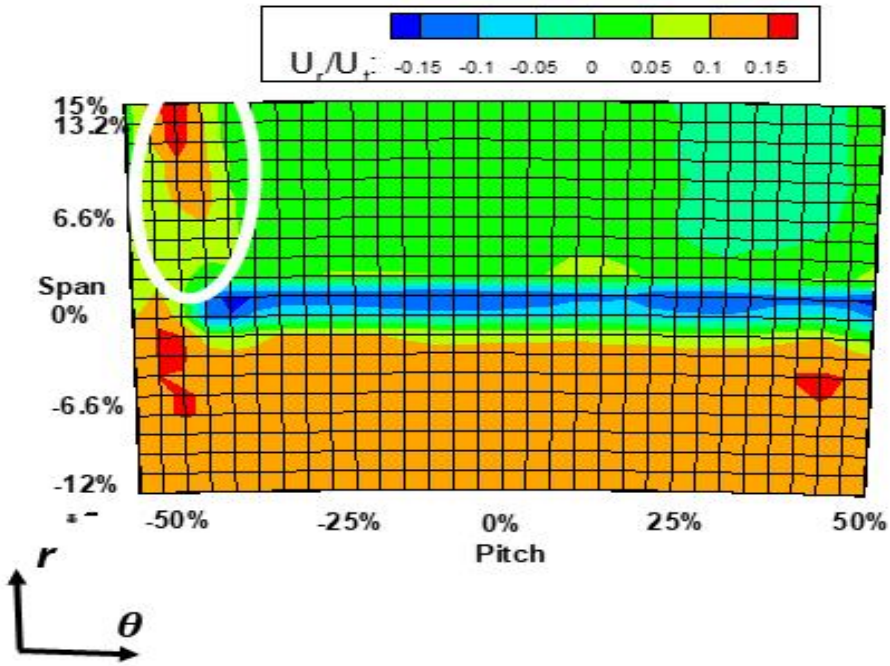

Figure 4.1.7 Radial-Tangential contour of Ur
Timestep 15/30

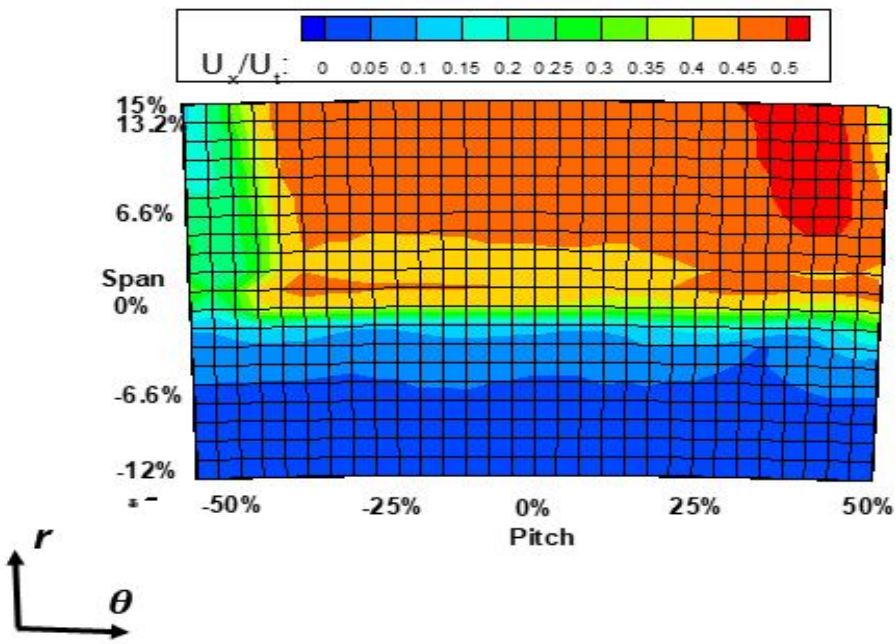

Figure 4.1.8 Radial-Tangential contour of Ux
Timestep 15/30

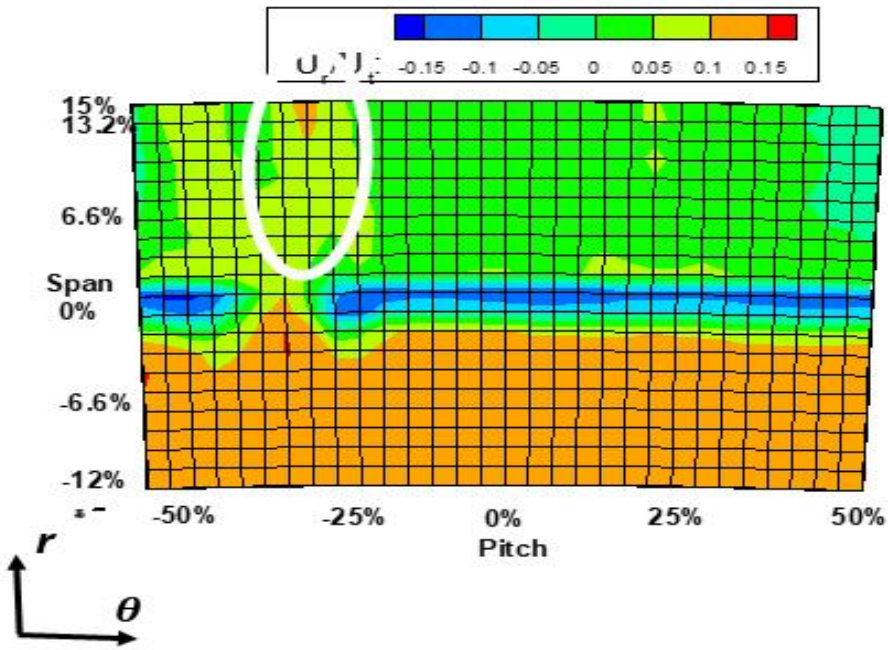

Figure 4.1.9 Radial-Tangential contour of Ur
Timestep 20/30

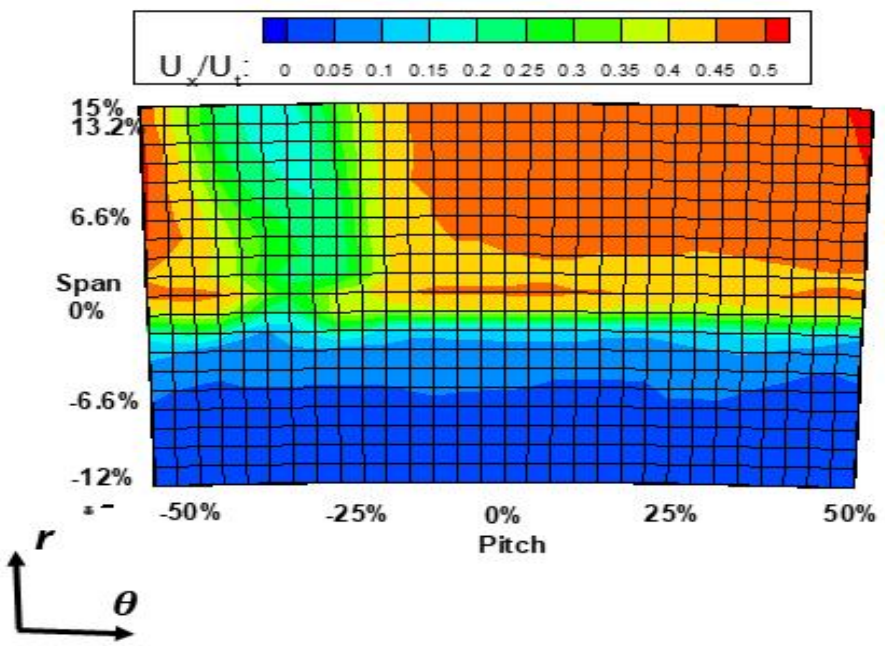

Figure 4.1.10 Radial-Tangential contour of Ux
Timestep 20/30

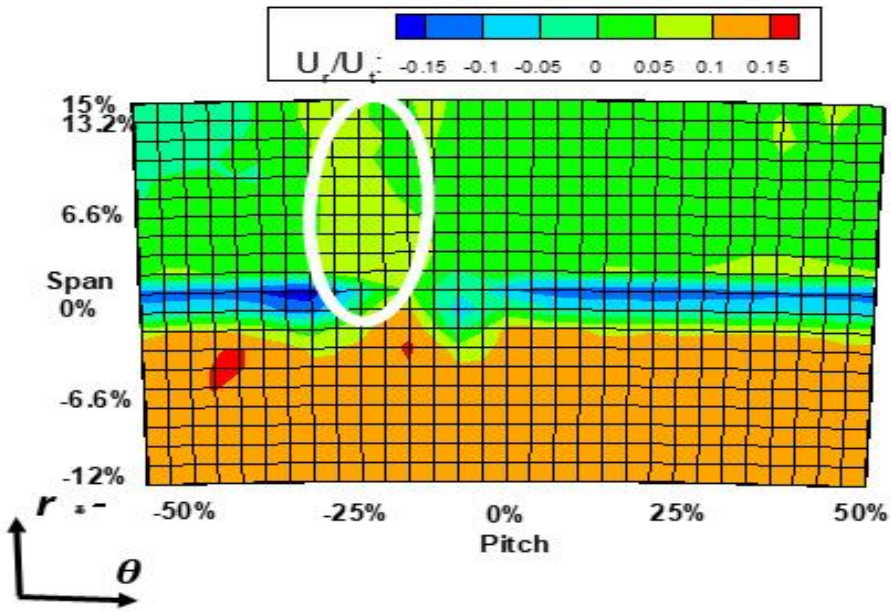

Figure 4.1.11 Radial-Tangential contour of Ur
Timestep 25/30

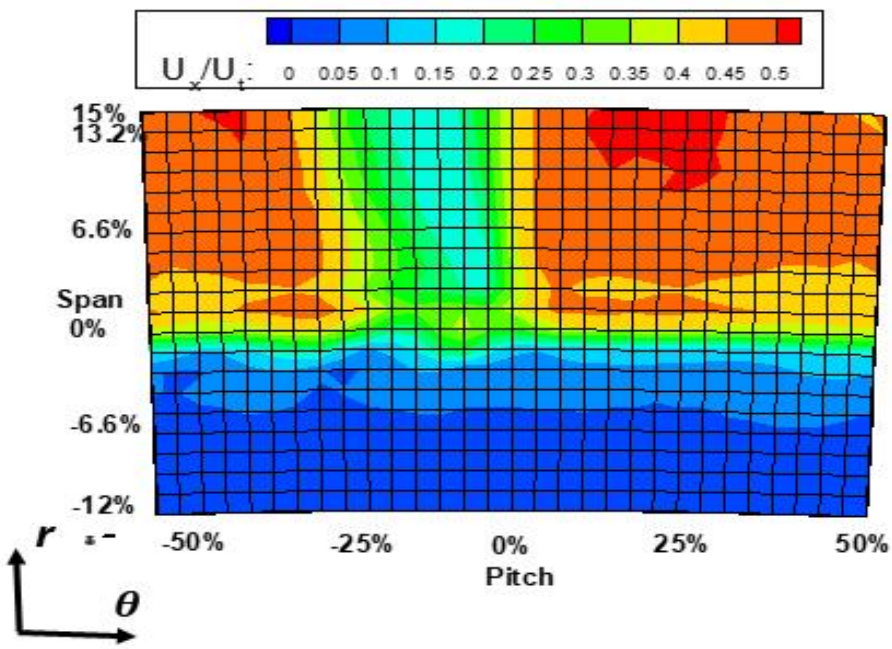

Figure 4.1.12 Radial-Tangential contour of Ux
Timestep 25/30

Figure 4.1.1 to 4.1.12 shows periodic unsteady phenomena of plane 5. (this phenomena occurs for all plane 5 to 1 so that only plane 5 is presented) Axial velocity contour represent region of upstream rotor wake and Radial velocity contour represent region of unsteady radial jet (white circle) behavior. Apparently periodic unsteady radial jet was generated and propagates with the same speed of the rotor wake. Thus the frequency of the unsteady radial jet is same with one rotor blade passing time. At the generation step(timestep 1/31), unsteady radial jet was generated at the hubside and as time goes by, unsteady radial jet propagates to the positive radial direction. At the same time its velocity magnitude is mitigating gradually.

On the other hand, cavity region has positive radial velocity for all the cavity. This is because plane 5 is very near to the cavity wall which rotate with the same speed of compressor shaft. Thus viscous disc pumping effect is major flow driving force.

However at the interface of cavity flow and main passage flow which is 0% of span, negative radial velocity is dominant which means flow mainly ingress to the cavity. On the other hand, at the below of the interface of cavity flow and main passage flow which is below 0% of span, there is zero radial velocity region which means at this region there is no radial direction flow velocity component.

It can be clearly observed that at the region unsteady where

radial jet present, radially positive directional(egress) velocity becomes stronger inside of the cavity. Clearly radically upward flow(egress) region moves with the same speed of the unsteady radial jet and rotor wake.

4.2. Ingress and Egress Pattern

4.2.1. Periodic Unsteady Ingress and Egress Pattern

(Axial Tangential plane - cavity mainstream interface-)

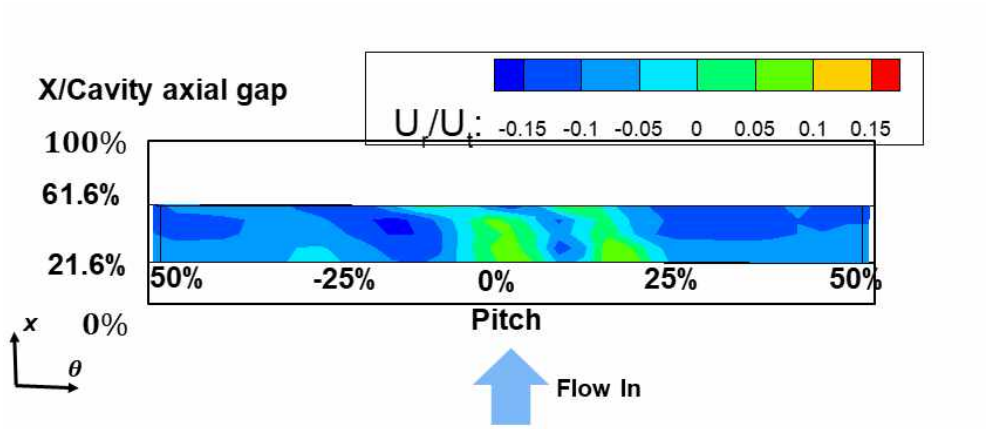

Figure 4.2.1 Axial-Tangential contour of Ur
Timestep 0/30

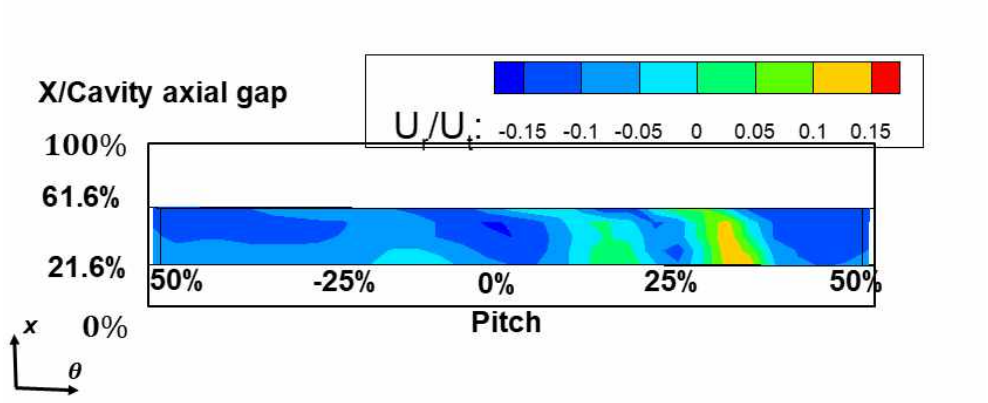

Figure 4.2.2 Axial-Tangential contour of Ur
Timestep 5/30

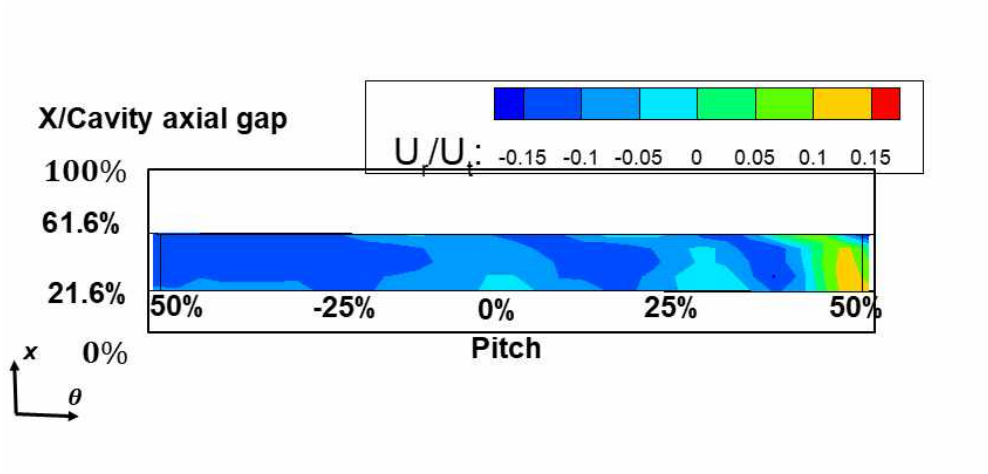

Figure 4.2.3 Axial-Tangential contour of Ur
Timestep 10/30

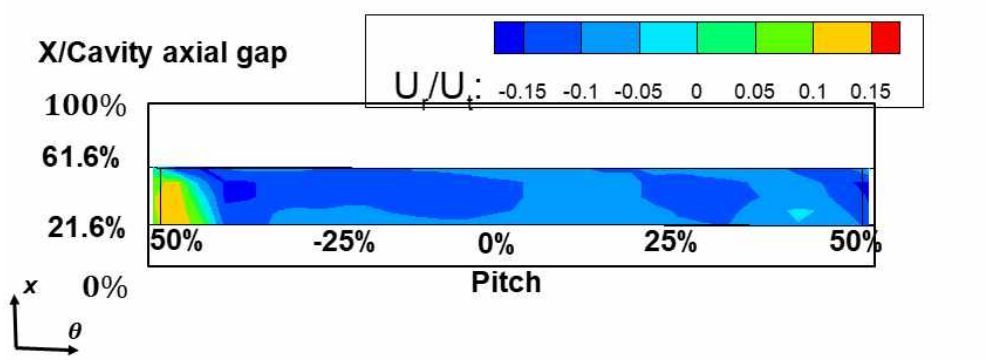

Figure 4.2.4 Axial-Tangential contour of Ur
Timestep 15/30

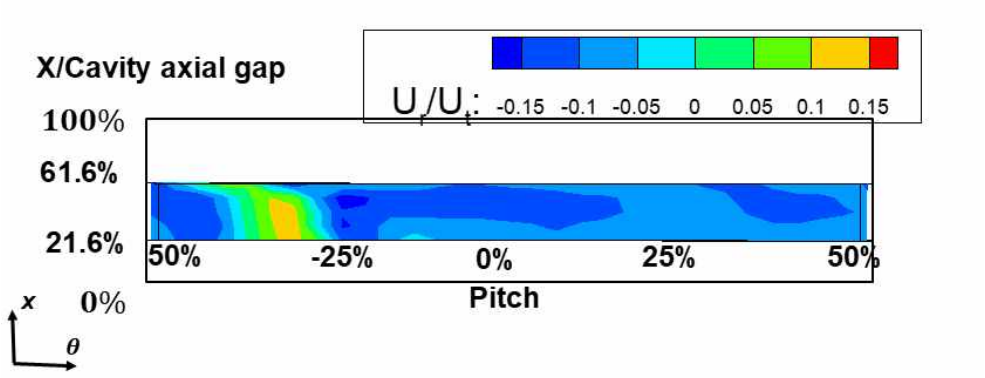

Figure 4.2.5 Axial-Tangential contour of Ur
Timestep 20/30

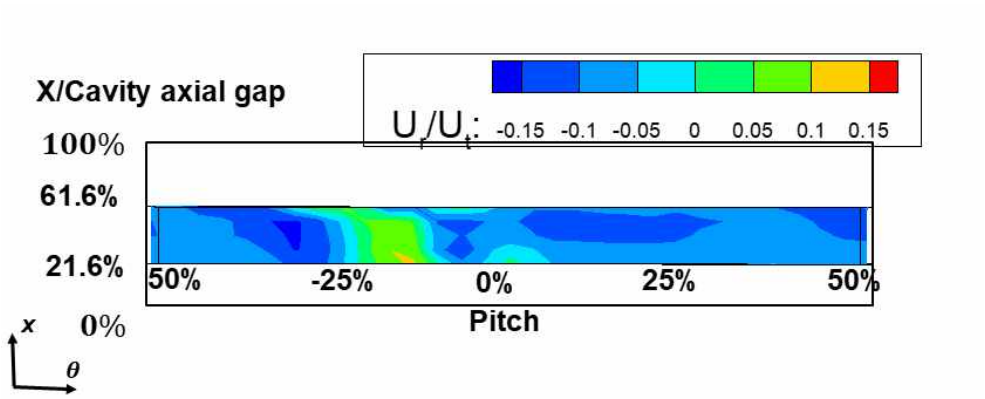

Figure 4.2.6 Axial-Tangential contour of Ur
Timestep 25/30

Figure 4.1.1 to 4.1.6 shows radial velocity distribution at radial=0 position which is interface of cavity and mainstream flow with different timesteps. Measured axial range which is 21.6% to 61.6% of axial gap has dominant negative velocity except for periodic unsteady radial jet effective region which moves as the speed of rotor. At the interface of the cavity and main flow region, negative radial velocity is dominant which means at the 21.6% to 61.6% of axial gap position, ingress to the cavity is major. Only the region where periodic unsteady radial jet region affecting has positive radial velocity which is egress from the cavity.

To sum up, at the interface of the cavity and main flow region ingress is dominant and as the periodic unsteady radial jet approaches ingress changes to egress. Moreover, it can be observed that periodic unsteady radial jet sweeps all pitch region and its axial effective range includes all measured plane in this study.

In these figures, generation and dissipation of radial jet can be easily recognized. Around pitch zero potion, periodic unsteady radial jet starts to generate and it moves to next blade passage and then start to dissipate. It looks like that when the newly generated periodic unsteady radial jet becomes largest and most powerful, old periodic unsteady radial jet completely disappear so that only one periodic unsteady radial jet exist. Generation to dissipation pitch

range is about one pitch. Also magnitude and range of periodic unsteady radial jet effect are stronger at the upstream of the measured plane than the downstream.

4.2.2. Time Averaged Ingress and Egress Pattern
(Axial Tangential plane - cavity mainstream interface-)

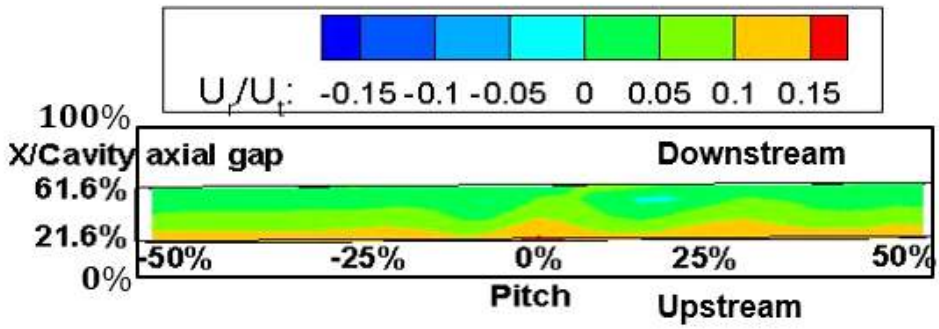

Figure 4.2.7 Time averaged radial velocity at -5% span

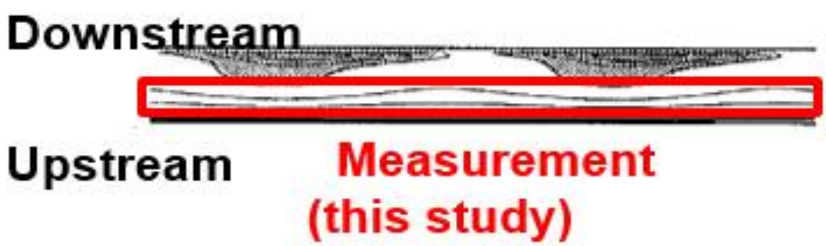

Figure 4.2.8 Steady calculation of radial velocity at -5% of span (white is cavity out direction) [10]

Figure 4.2.7 shows time averaged radial velocity at -5% span position and figure 4.2.8 shows steady calculation of radial velocity at -5% of span. This two figures ingress or egress at the position can be determined. Position of interest is determined by the data from previous research of wellborn[10]. By this figure, When the time averaged radial velocity is compared with the previous steady

calculated data of previous research at the same position(-5% span), although wellborn does not gives quantitative value, it is well matched with previous research qualitatively. Both of which has dominant positive radial velocity(egress) and as the position approaches to the upstream magnitude of ingress becomes larger. This is because cavity upstream wall is rotating and disc pumping effect is dominant at the vicinity of cavity upstream wall.

However the measurement range of this study is from 21.6% to 61.6% of axial gap, ingress pattern which can be recognized at the wellborn's data can not be obtained.

4.3. Periodic Unsteady Flow Structure at the Cavity

4.3.1. Periodic Unsteady Radial Jet and Radial Axial Plane Flow Field.

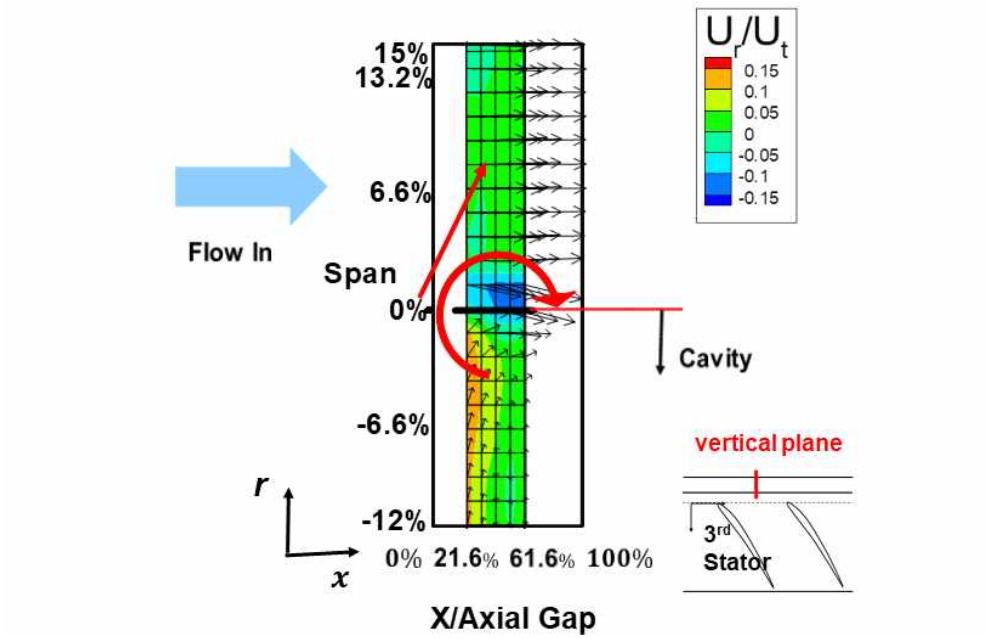

Figure 4.3.1 Axial-Radial contour of Ur and velocity vector Timestep 0/30

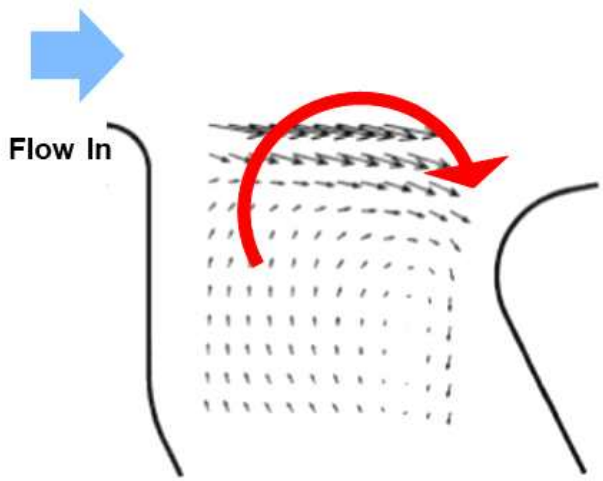

Figure 4.3.2 Steady calculation of Wellborn Axial-Radial contour of velocity vector

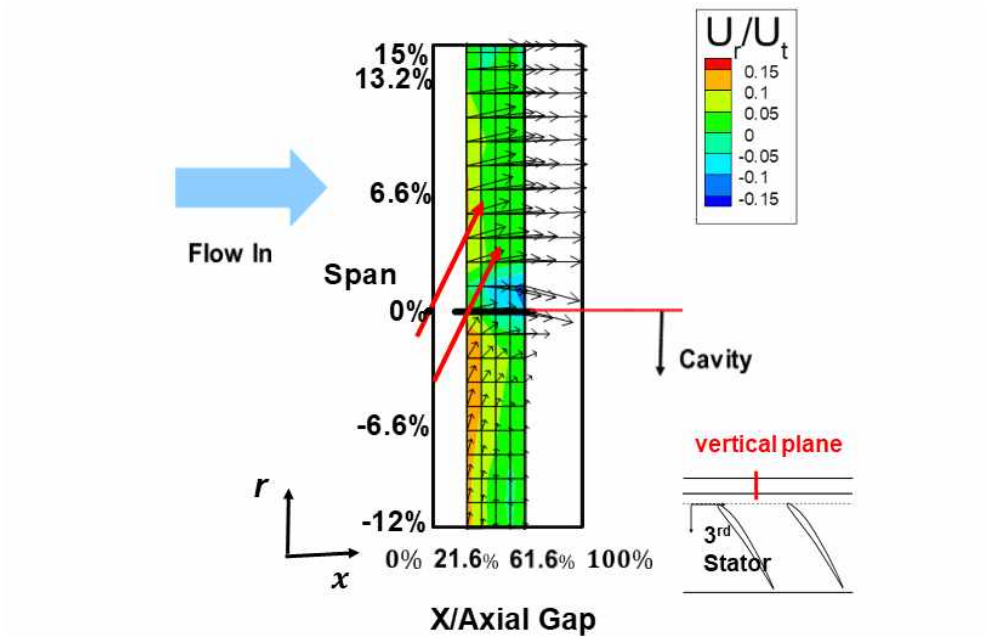

Figure 4.3.3 Axial-Radial contour of Ur and velocity vector Timestep 1/30

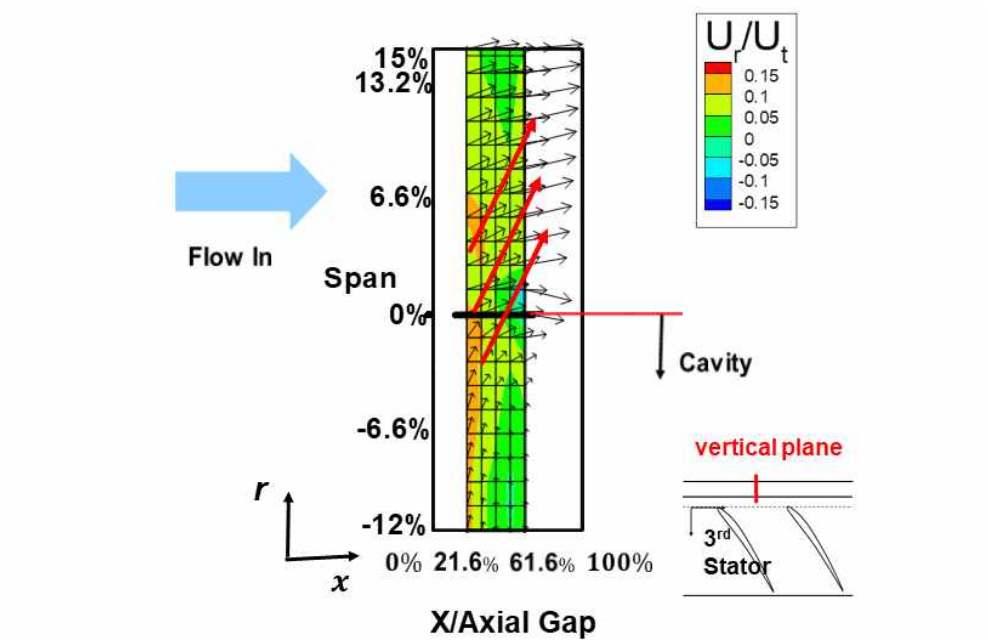

Figure 4.3.4 Axial-Radial contour of Ur and velocity vector Timestep 2/30

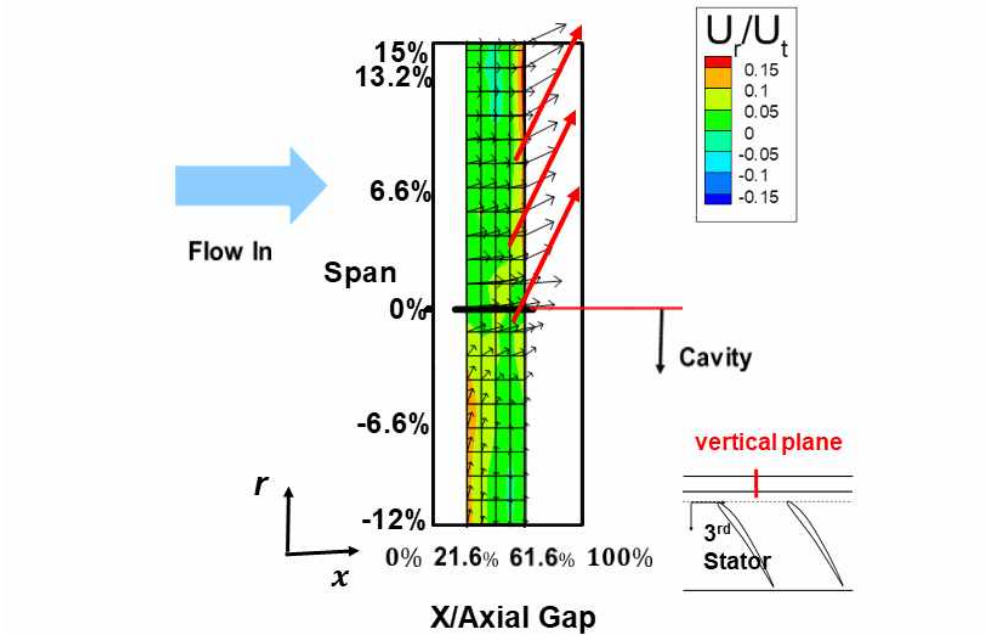

Figure 4.3.5 Axial-Radial contour of Ur and velocity vector Timestep 3/30

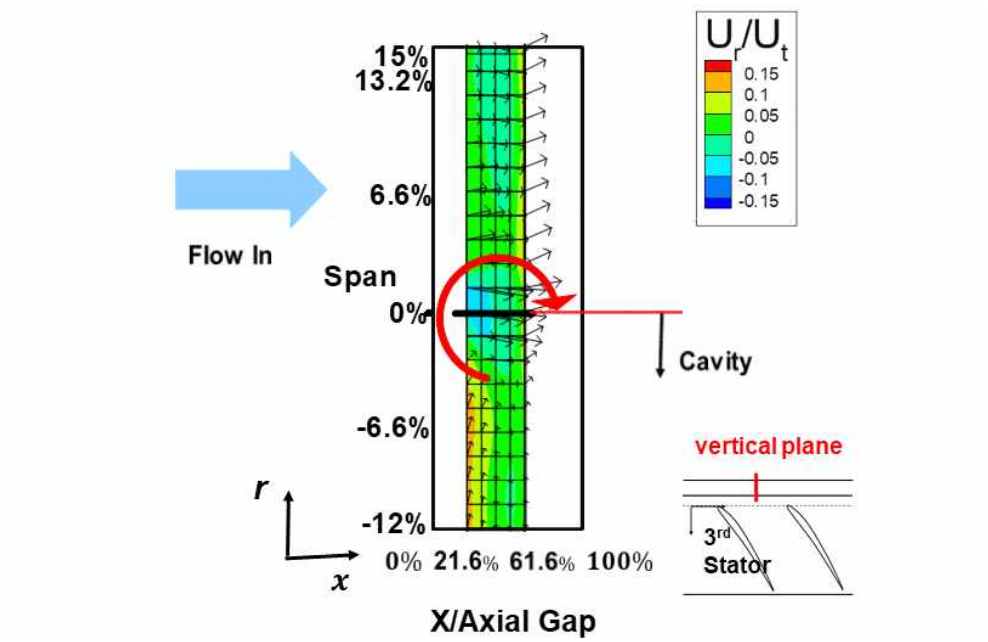

Figure 4.3.6 Axial-Radial contour of Ur and velocity vector Timestep 4/30

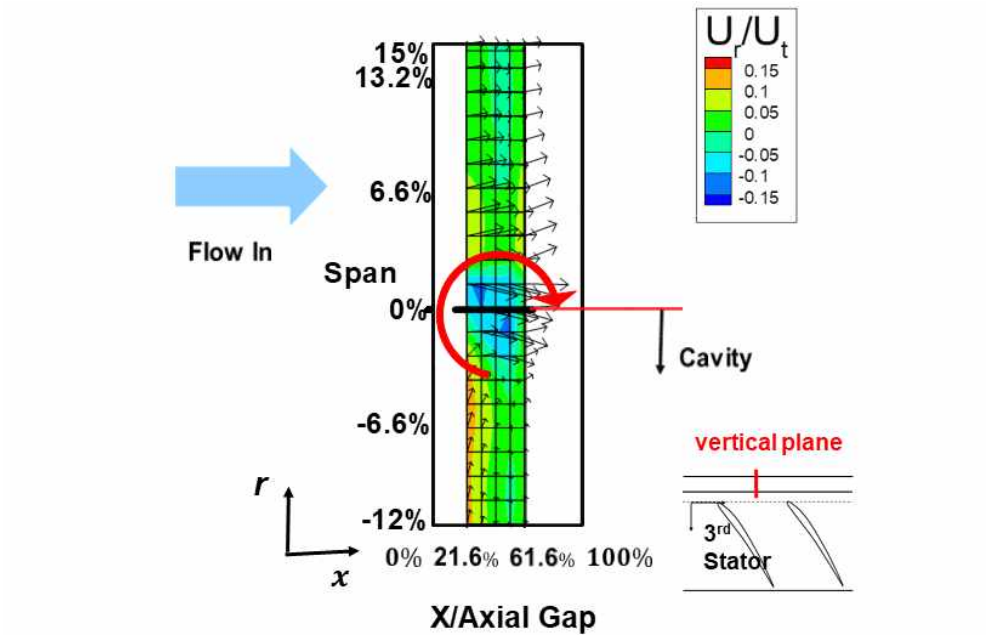

Figure 4.3.7 Axial-Radial contour of Ur and velocity vector Timestep 5/30

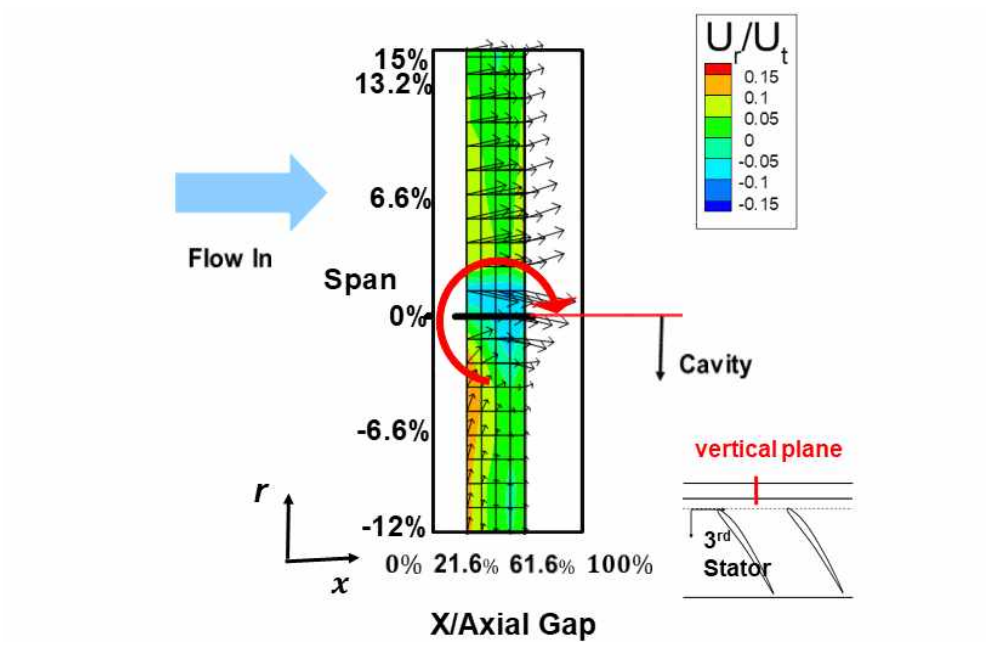

Figure 4.3.8 Axial-Radial contour of Ur and velocity vector Timestep 6/30

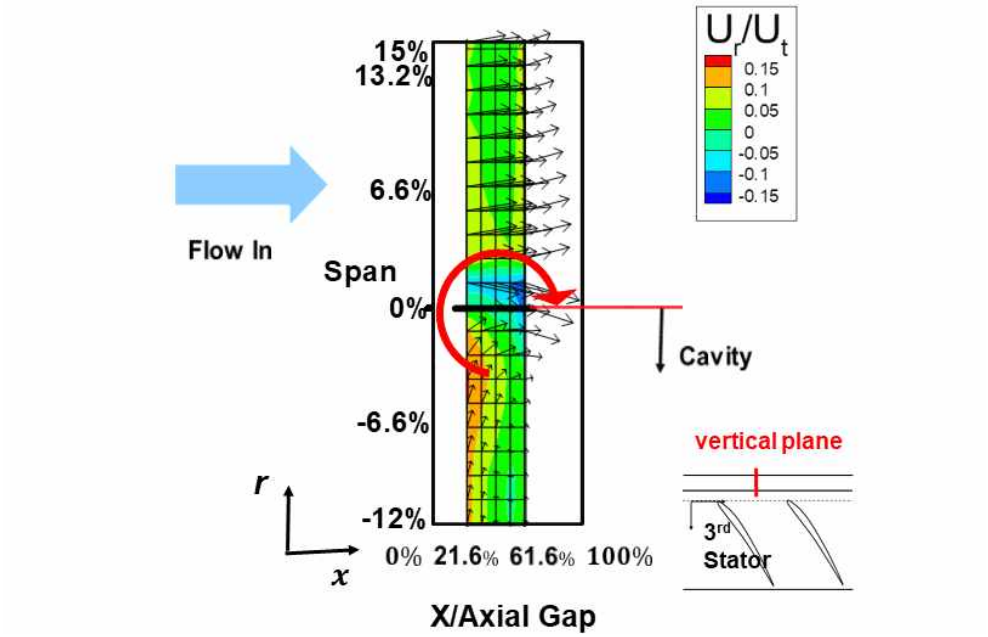

Figure 4.3.9 Axial-Radial contour of Ur and velocity vector
Timestep 7/30

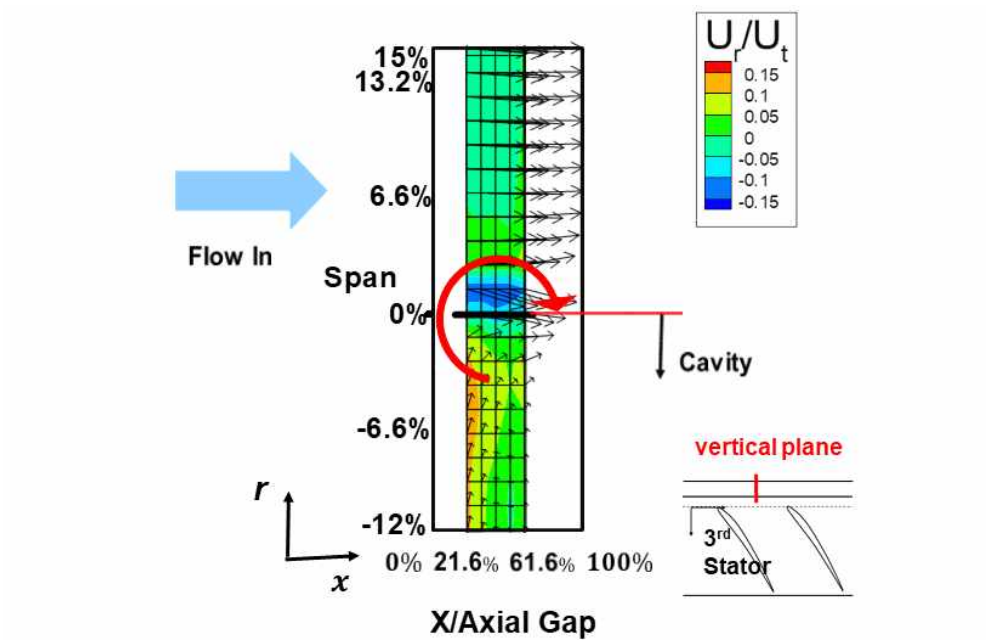

Figure 4.3.10 Axial-Radial contour of Ur and velocity vector
Timestep 10/30

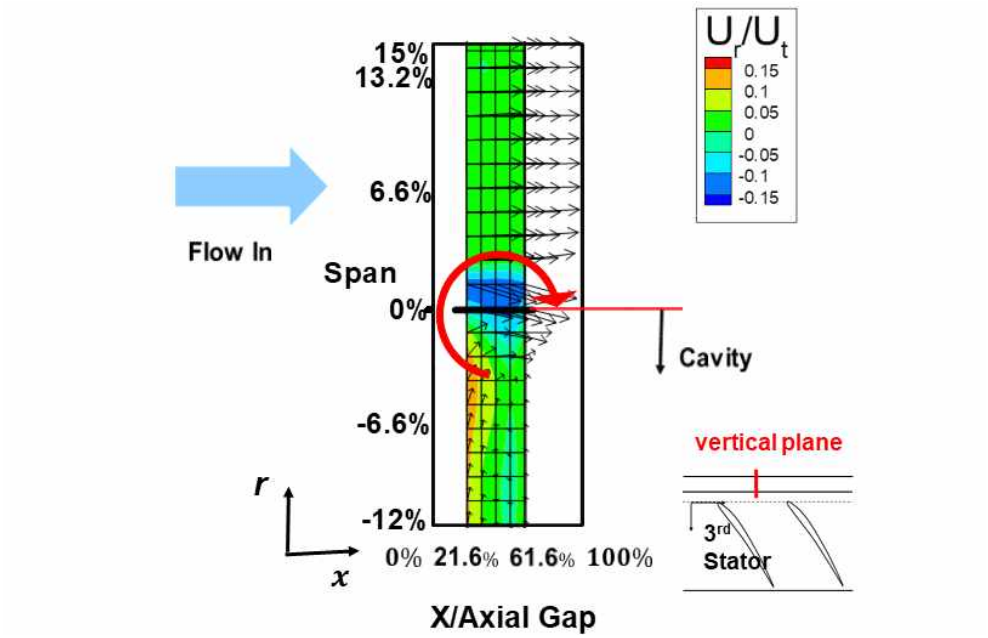

Figure 4.3.11 Axial-Radial contour of Ur and velocity vector Timestep 15/30

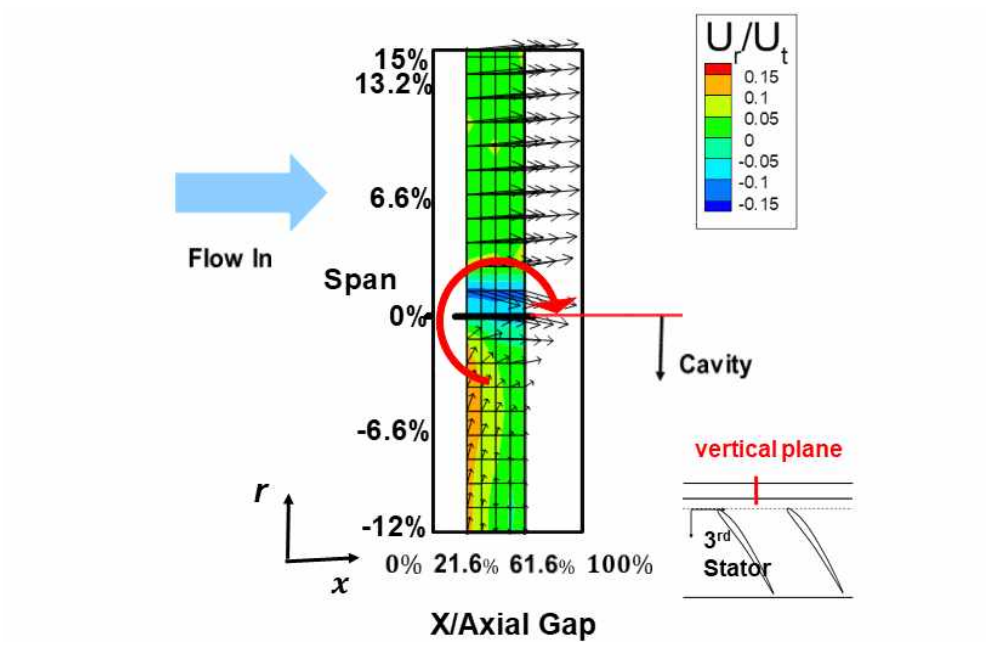

Figure 4.3.12 Axial-Radial contour of Ur and velocity vector Timestep 20/30

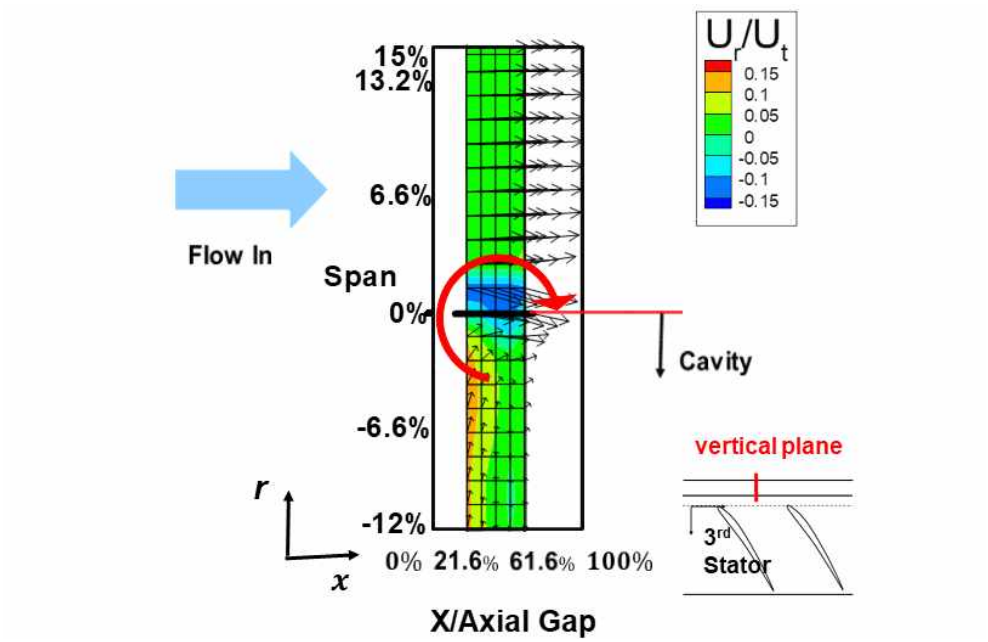

Figure 4.3.13 Axial-Radial contour of Ur and velocity vector
Timestep 25/30

At the figure 4.3.1 to 4.3.13, color contour represent radial velocity magnitude and arrow represent velocity vector at the axial radial plane. Assuming that flow very near the cavity upstream wall only has radial directional component, flow has certain partial circular structure just like previous research of welborn[10] for the all time steps except for the time step when periodic radial jet present.

When periodic radial jet start to approaches which is figure 4.3.3, the circular structure start to change. the structure becomes to has more radial velocity components and overall flow structure position change to radially upward and axially downstream direction. After that as the periodic unsteady radial jet moves with the rotor blade

and it became to has more effect on the cavity flow structure. At the figure 4.3.4 which is next time step of figure 4.3.3, periodic unsteady radial jet core position align with our plane of interest, partial circular structure inside of cavity is destroyed completely and radial upward direction flow(egress) becomes dominant for all measured position inside of the cavity. At the next time step which is figure 4.3.5, periodic unsteady radial jet moves to the downstream, however still radial upward direction flow dominant.

In the figure 4.3.6 which is next time step of figure 4.3.5, radial upward direction flow propagate to downstream and almost disappear in the plane of interest. Align with disappearance of radial upward direction flow, partial circular structure start to appear at the vicinity of the cavity upstream wall.

At the next time step which is figure 4.3.7, partial circular structure become to appear with complete form. The regained partial circular structure consists for all time steps after that although the position of the circular structure fluctuate with as main passage flow structure changes.

Thus not like steady simulation of previous research, main effect on the flow structure inside cavity is main passage flow structure. Moreover partial circular structure is not a universal thing because its structure can be destroyed by the main flow structure which is radial upward direction flow in this study. Cavity flow is major loss

source of the shrouded type stator and radial upward direction flow to cavity flow interaction must be considered at the design step of a compressor.

4.3.2. Sudden Expansion, Disc Pumping and Pressure Difference Effect Near the Cavity

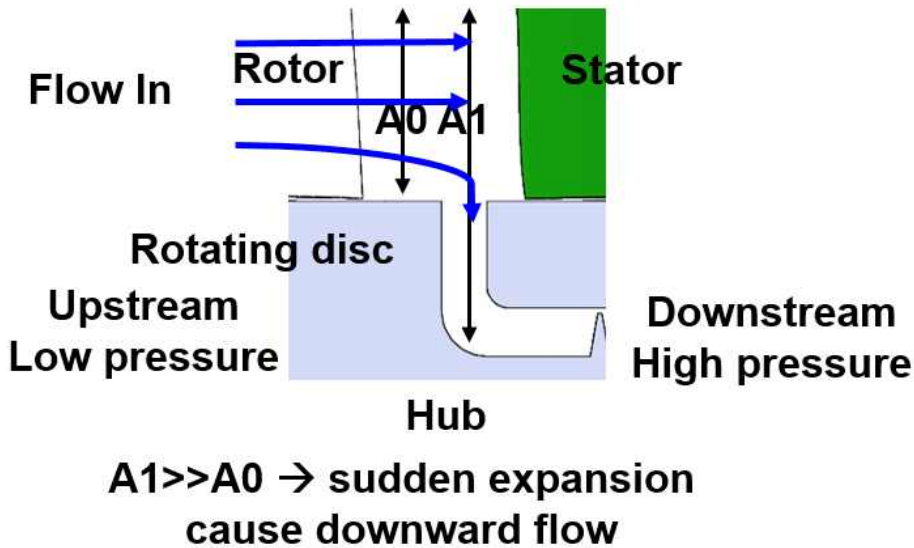

Figure 4.3.14 Configuration of sudden area expansion effect, axial-radial view

According to fugure 4.3.1 to 4.3.13 ingress flow is dominant at the interface of cavity flow and main passage flow. This phenomena can be explained by sudden of cross section area of flow. When the incoming flow approaches to the cavity, at the hubside of the main flow, cross sectional area suddenly expands. Thus the flow which has streamline near the hubside ingress to the cavity.

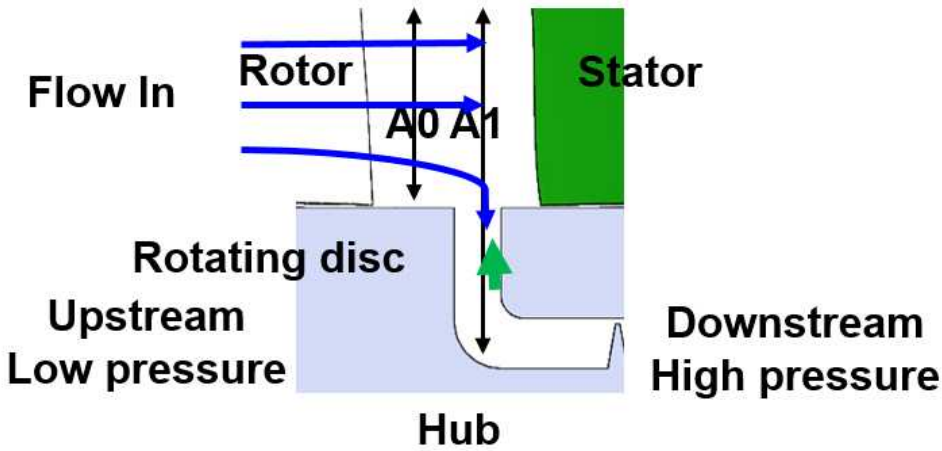

Figure 4.3.15 Configuration of sudden area expansion effect and pressure difference effect, axial-radial view

As figure 4.3.15 represent, ingress flow can not ingress to the cavity completely because in a compressor stator downstream flow has higher static pressure than stator upstream, flow recirculate from downstream to upstream through cavity and this direction is egress direction. Thus egress flow caused by higher downstream static pressure crush with ingress flow caused by sudden expansion of main flow making interface of cavity flow and main flow.

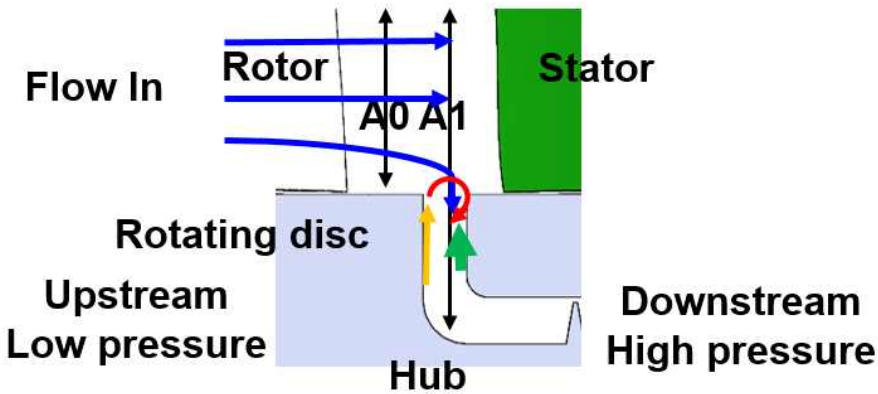

Figure 4.3.16 Configuration of sudden area expansion effect, disc pumping effect, and pressure difference effect, axial-radial view

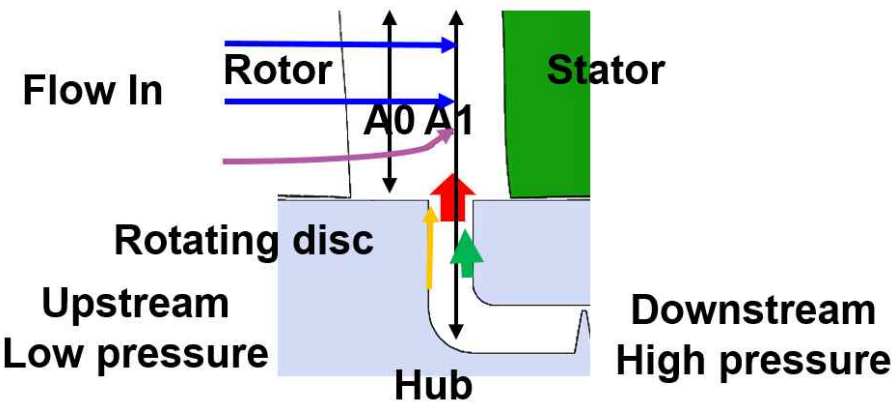

Figure 4.3.17 Configuration of cavity flow when periodic unsteady radial jet present, axial-radial view

However, just like the configuration of 4.3.14, sudden expansion effect(marked by blue arrow) and pressure difference effect(marked by green arrow) are not the only which affect the overall partial circular flow structure. Egress flow near the rotating disc is also exist, which is called as disc pumping effect. When the disc rotates, flow particle which located near the disc affected by centrifugal force

so that the flow moves outward to the cavity.

Thus partial circular flow structure in this study can be explained by pressure difference, disc pumping, sudden expansion effect. At the hubside, when flow approaches to the cavity flow experience sudden expansion. So the flow ingress to the cavity. However the flow can not ingress to the cavity completely because of pressure difference effect and radial zero velocity component zone is generated. On the other hand, very vicinity to the cavity upstream wall which rotate with the same speed of the compressor shaft, disc pumping effect is dominant. Thus at the cavity upstream wall region even though this study only has axial measurement region of 21.6% to 61.6% of axial gap region, it is easily supposed that egress may dominant upstream of 21.6% of axial gap.

But at the time step when periodic unsteady radial jet is present, partial circular flow structure is destroyed and only egress present. This is because when periodic unsteady radial jet is approached, magnitude of radially positive velocity component caused by periodic unsteady radial jet is very large and it exceeds the magnitude of radially negative velocity component caused by sudden expansion effect.

4.4. Upstream and Downstream of cavity

4.4.1. Cavity Upstream Radial Tangential Plane (plane U)

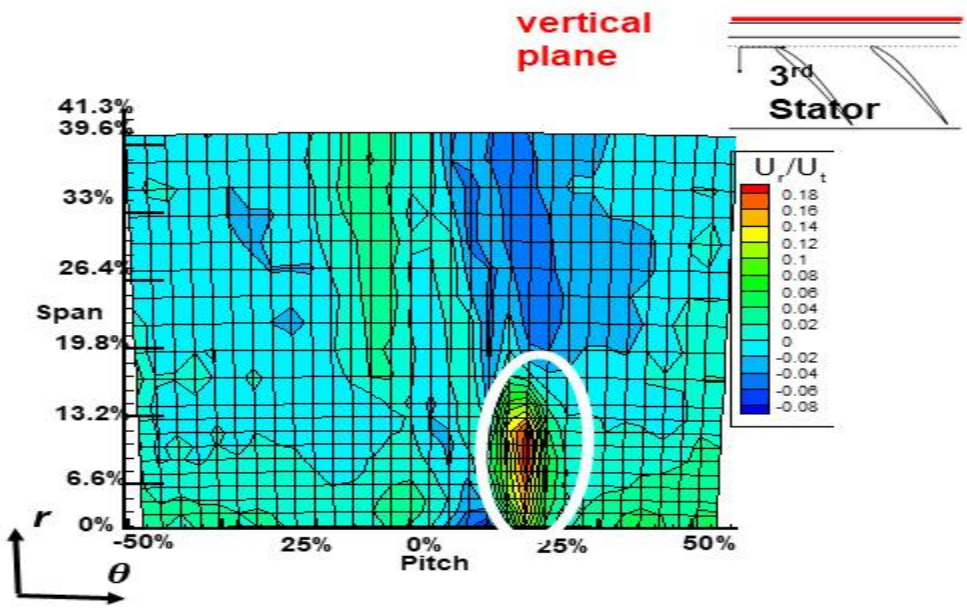

Figure 4.4.1 Radial-Tangential contour of Ur
Timestep 0/30

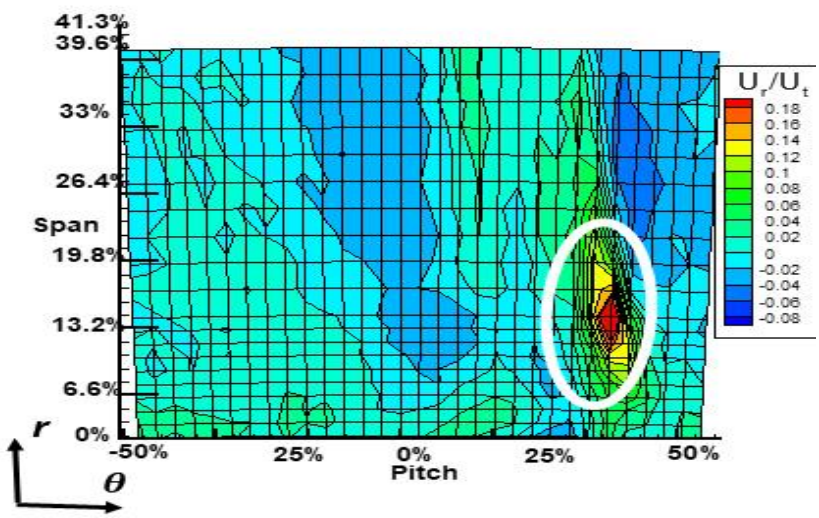

Figure 4.4.2 Radial-Tangential contour of Ur
Timestep 5/30

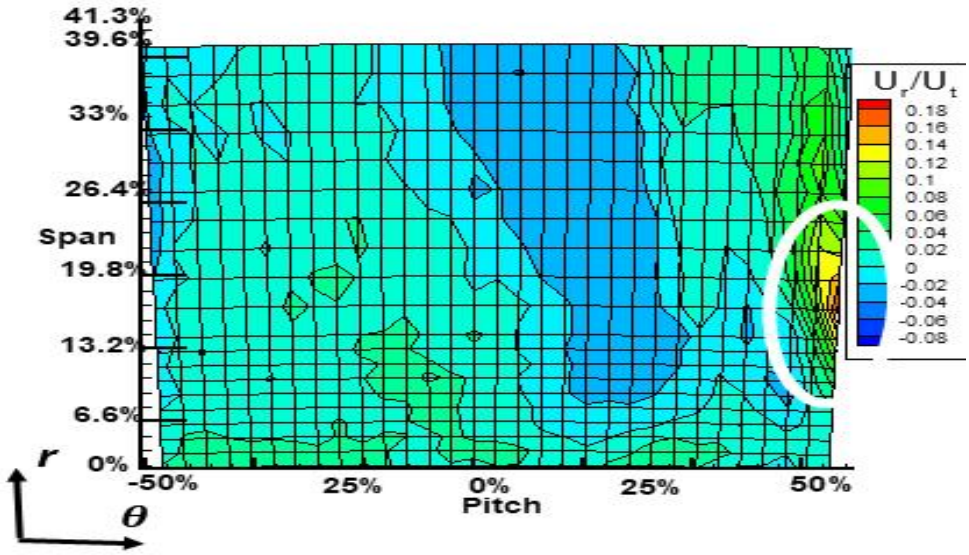

Figure 4.4.3 Radial-Tangential contour of Ur
Timestep 10/30

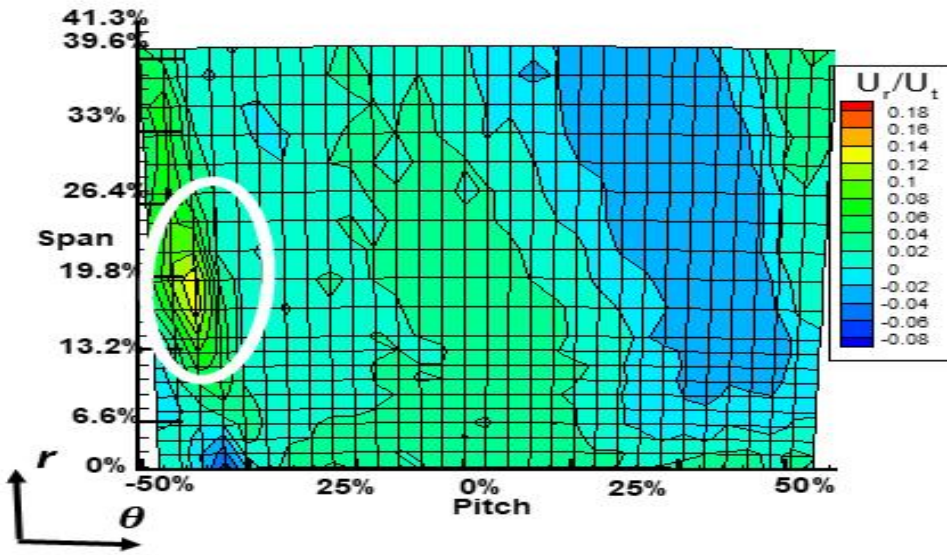

Figure 4.4.4 Radial-Tangential contour of Ur
Timestep 15/30

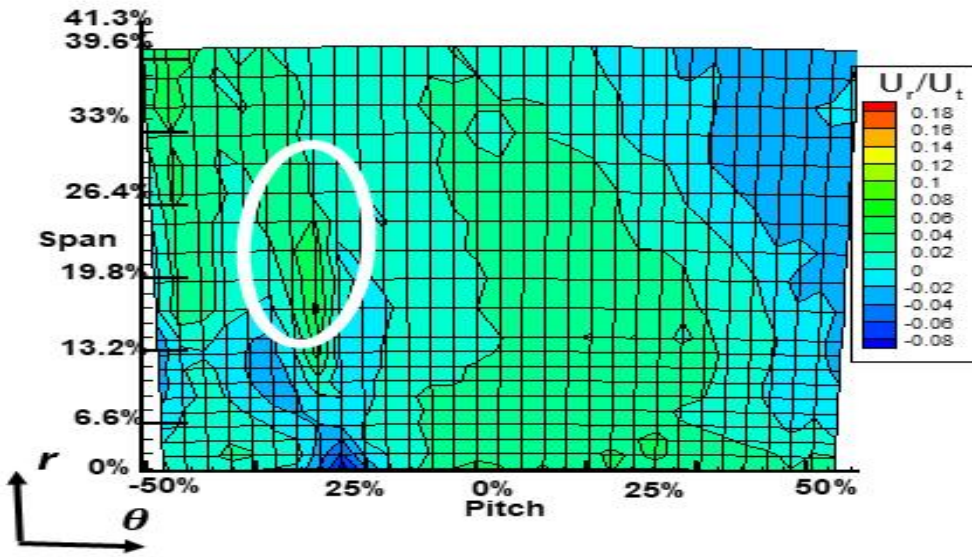

Figure 4.4.5 Radial-Tangential contour of Ur
Timestep 20/30

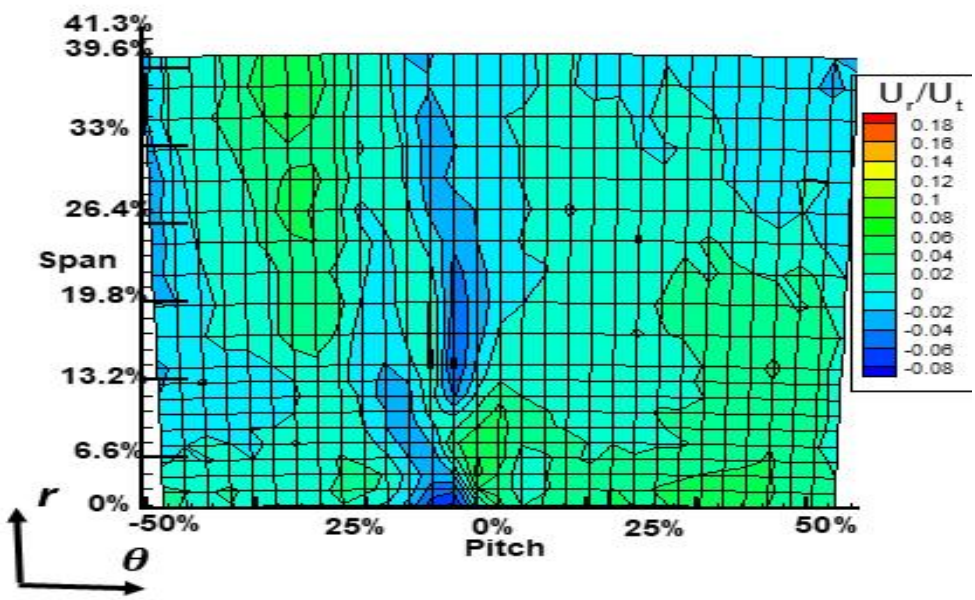

Figure 4.4.6 Radial-Tangential contour of Ur
Timestep 25/30

Figure 4.1.4 to 4.1.6 shows periodic unsteady phenomena of plane U. Radial velocity contour represent region of unsteady radial jet (white circle) behavior. Just like cavity region planes, periodic unsteady radial jet was generated and propagates with the same speed of the rotor wake(not presented here). Also periodic unsteady radial jet generated at the hubside and it moves to the casing direction. Radial effective range of periodic unsteady radial jet exceeds the measured exceeds 39.6% of the span.

Not like the case of cavity region, periodic unsteady radial jet at the plane U completely disappear at the time step 26 which is figure 4.4.6.

Most interesting part of plane U is that even though plane U dose not have any cavity region, still periodic unsteady radial jet present so that it can be concluded that periodic unsteady radial jet occurs without cavity.

4.4.2. Cavity Downstream Radial Tangential Plane (plane D)

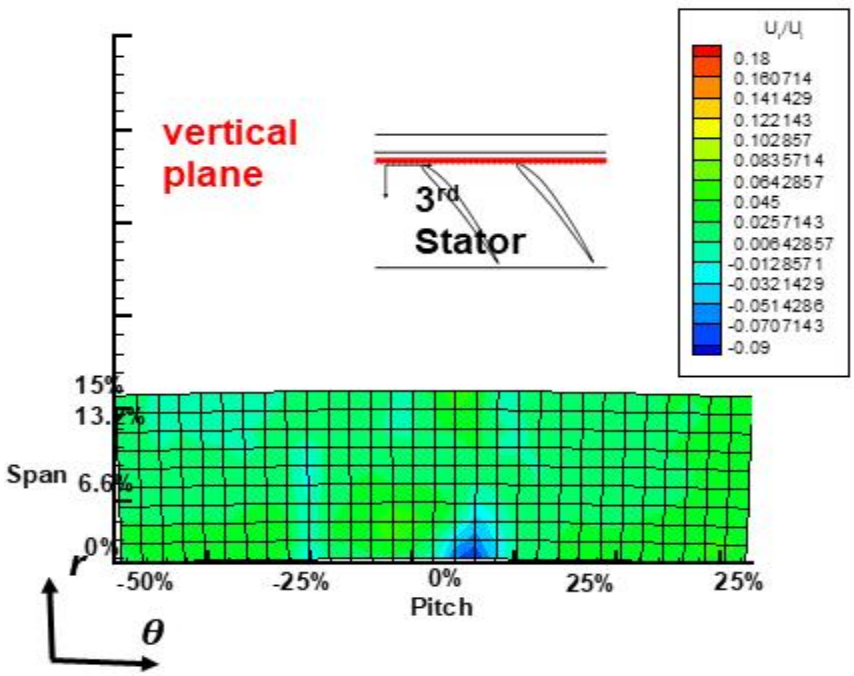

Figure 4.4.7 Radial-Tangential contour of Ur
Timestep 0/30

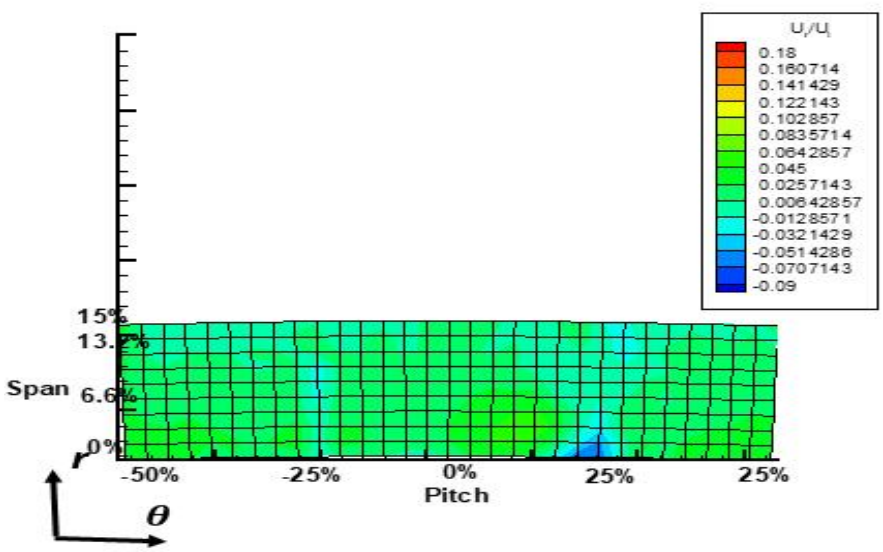

Figure 4.4.8 Radial-Tangential contour of Ur
Timestep 5/30

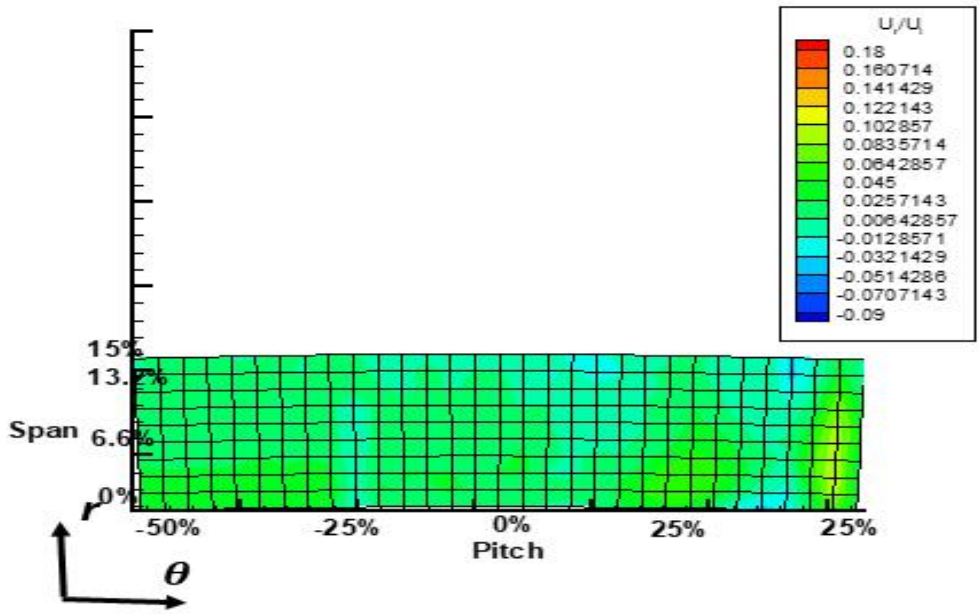

Figure 4.4.9 Radial-Tangential contour of Ur
Timestep 10/30

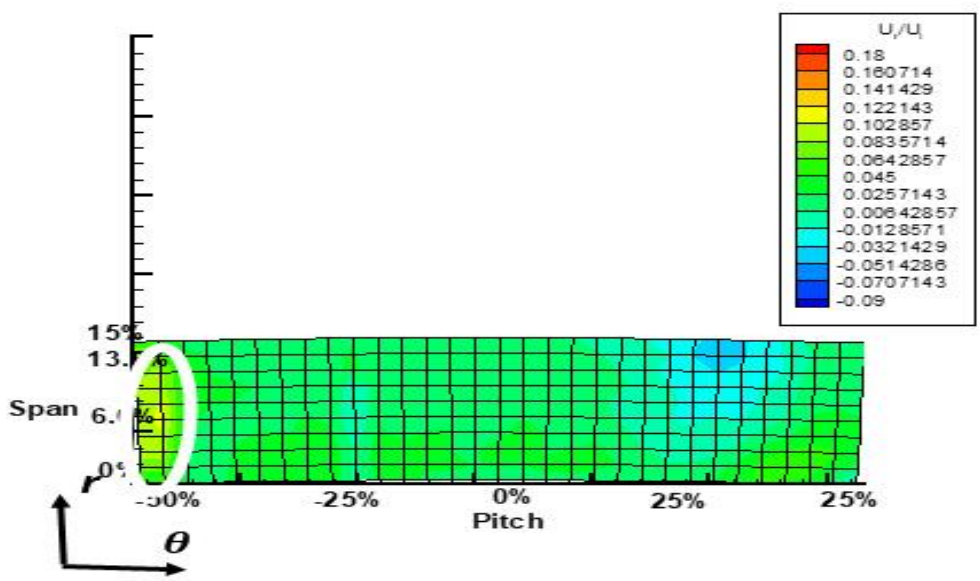

Figure 4.4.10 Radial-Tangential contour of Ur
Timestep 15/30

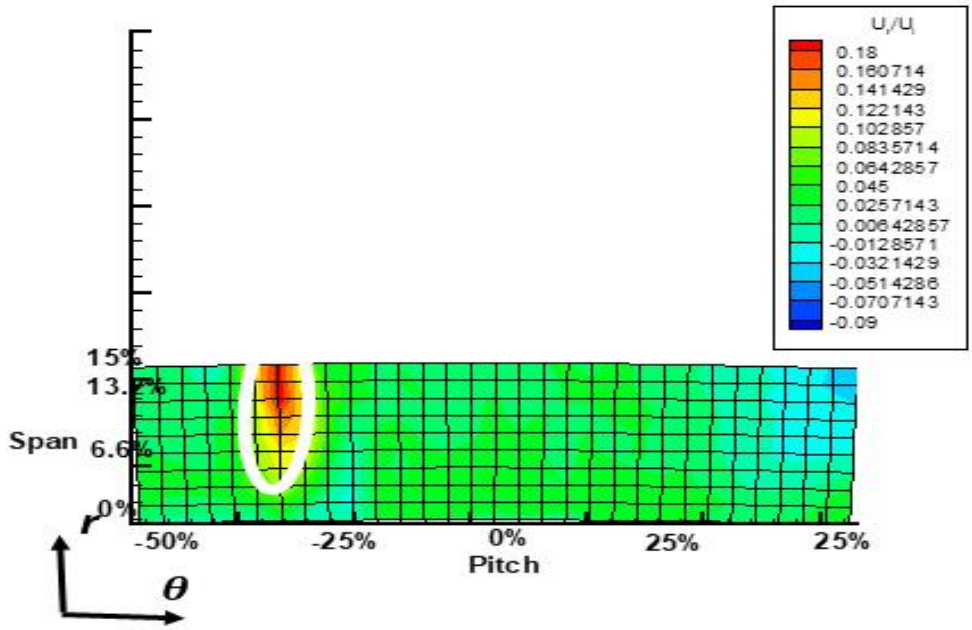

Figure 4.4.11 Radial-Tangential contour of Ur
Timestep 20/30

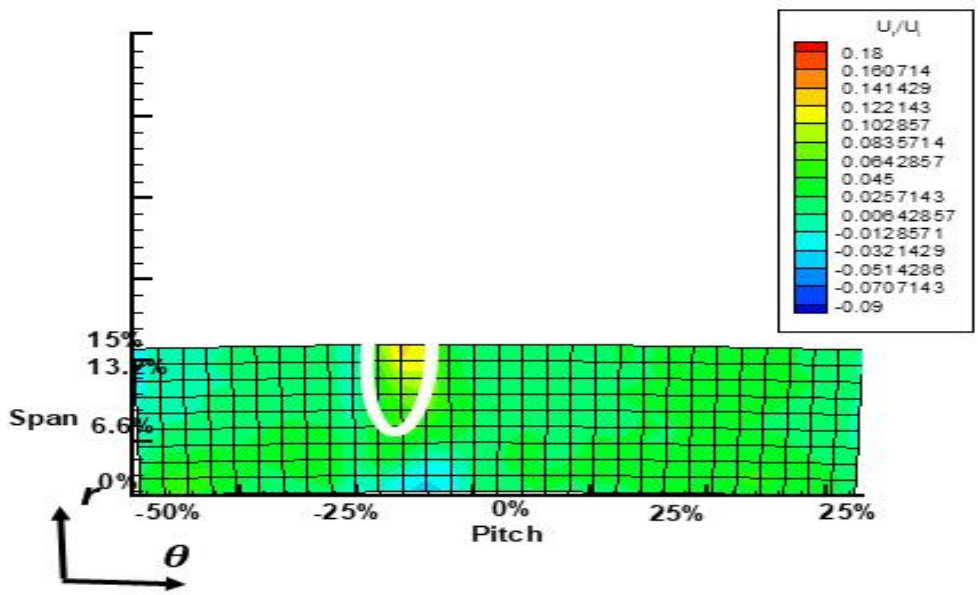

Figure 4.4.12 Radial-Tangential contour of Ur
Timestep 25/30

Figure 4.1.7 to 4.1.12 shows periodic unsteady phenomena of plane D. Radial velocity contour represent region of unsteady radial jet (white circle) behavior. Periodic unsteady radial jet was propagates with the same speed of the rotor wake(not presented here). However, not like cavity region planes and upstream plane, periodic unsteady radial jet does not be observed at all time step. Periodic unsteady radial jet can be identified only 15/30 to 25/30 time step which are the time steps powerful periodic unsteady radial jet exist at the cavity region planes and upstream plane.

However time steps when periodic unsteady radial jet can be identified, periodic unsteady radial jet is still powerful and it is likely to propagate to the next stage. Thus when designing blade periodic unsteady radial jet should be considered.

Chapter 5. Conclusions

Unsteady three dimensional velocity measurement in a shrouded upstream cavity and adjacent passage has been conducted for the first time to investigate cavity flow to main flow interaction.

1. Periodic unsteady radial jet is the main factor which makes difference between phase locked ensemble averaged data and steady data.

2. Periodic unsteady radial jet moves with the same speed of the rotor wake with periodic generation and dissipation.

3. At the interface of cavity flow and main passage flow which is 0% of span, negative radial velocity(ingress) is dominant.

4. However when periodic unsteady radial jet approaches, radially positive directional(egress) velocity becomes dominant inside of the cavity.

5. Time averaged data of this study coincide with steady simulation of previous research.

6. Flow inside of cavity has certain partial circular structure just like previous research for the most of the time, however as periodic radial jet approaches, the structure destroyed and egress become dominant.

7. Periodic unsteady radial jet exist upstream and downstream of cavity.

8. Also periodic unsteady radial jet propagates to the next stage, it should be considered at the designing step of a compressor.

Bibliography

[1] Yoon, S., Selmeier, R., Cargill, P., Wood, P., 2014, “Effect of the Stator Hub Configuration and Stage Design Parameters on Aerodynamic Loss in Axial Compressors,” ASME Turboexpo 2014, GT2014-26905.

[2] Wellborn, S. R. and Okiishi, T. H., “Effects of Shrouded Stator Cavity Flows on Multistage Axial Compressor Aerodynamic Performance.” NASA CR 198536, October 1996.

[3] Hedegger, N. J., Hall, E. J, and Delaney, R. A., “Parameterized Study of High-Speed Compressor Seal Cavity Flow,” AIAA Paper 96-2807, July 1996.

[4] Lange, M., Mailach, R., Vogeler, K., 2010, “An Experimental Investigation of Shrouded and Cantilevered Compressor Stators at Varying Clearance Sizes,” ASME Turboexpo 2010, GT2010-22106.

[5] Kato, D., Yamagami, M., Tsuchiya, N., Komada, H., 2011, “The Influence of Shrouded Stator Cavity Flows on the Aerodynamic Performance of a High-Speed Multistage Axial Compressor,” ASME Turboexpo 2011, GT2011-46300.

[6] Mailach, R., Lehmann, I., Vogeler, K., 2008b, “Periodical Unsteady Flow Within a Rotor Blade Row of an Axial

Compressor - Part II: Wake-Tip Clearance Vortex Interaction," Journal of Turbomachinery, Vol. 130 (4), 041005.

[7] Montomoli, F., Naylor, E., Hodson, H. P., Lapworth, L., 2013, "Unsteady Effects in Axial Compressors: A Multistage Simulation," Journal of Propulsion and Power, Vol. 29

[8]Streamline© / Streamware© Installation & Users guide, Vol.3, Dantec Dynamics, Denmark, Retrieved from https://www.dantecdynamics.com/

[9] Shin, H. W., Whitfield, C. E., Wisler, D. C., 1994, "Rotor-Rotor Interaction for Counter-Rotating Fans, Part 1: Three-Dimensional Flowfield Measurements," AIAA Journal, Vol. 32 (11), pp.2224-2233.

[10] Wellborn, S. R., 2001, "Details of Axial-Compressor Shrouded Stator Cavity Flows," ASME Turboexpo 2001, 2001-GT-0495.

[11] Kim, J. W., and Song, S. J. "Effects of Seal Cavity Flows on the Aerodynamic Performance in a Shrouded Compressor Stator Passage," Ph.D Thesis, 2011.

[12] Pfau, A., Schlienger, J., Rusch, D., Kalfas, A. I., Abhari, R. S., "Unsteady Flow Interactions Within the Inlet Cavity of a Turbine Rotor Tip Labyrinth Seal," Journal of Turbomachinery,

October 2005.

[13] Denton, J. D., 2010, “Some Limitations of Turbomachinery CFD,” ASME Turboexpo 2010, GT2010-22540.

초 록

축류압축기 슈라우드 상류 캐비티 내부 유동과 주 요동의 상호작용을 연구하기 위해 캐비티 내부, 그리고 캐비티와 인접한 주 유로에서 앙상블 평균된 삼차원 속도 벡터를 측정하였다. 삼차원 속도장을 얻기 위하여 일차원 열선을 세 번의 요(Yaw) 방향에서 측정하였다. 앙상블 평균된 속도장과 정상 속도장의 가장 큰 차이점은 방사상의 주기적 비정상 제트 유동이었다. 이 유동은 동익 웨이크와 같은 속도로 이동하며 발생과 소멸을 주기적으로 거듭하였다. 이 연구에서 캐비티 유동과 주 유동의 경계에서는 캐비티 안쪽으로 향하는 유동이 우세하였다. 하지만 주기적 비정상 제트 유동이 접근하면 캐비티 바깥쪽으로 향하는 유동이 우세하게 순간적으로 변하였다. 또한, 본 연구의 시간 평균된 속도장은 이전의 연구에서 계산되었던 정상 속도장과 부합하였다. 캐비티 내부의 유동은 대부분의 시간 동안 특정한 원주의 일부 같은 형상을 띠고 있지만, 주기적 비정상 제트 유동이 접근함에 따라서 캐비티 바깥쪽으로 향하는 유동으로 변한다. 또한, 주기적 비정상 제트 유동은 슈라우드 상류 캐비티의 상류와 하류 모두에 존재하며 다음 단으로 전파되기에 압축기 설계 단계에서 주기적 비정상 제트 유동을 고려해야 한다.

주 요 어: 축류압축기, 주기적 비정상 측정, 슈라우드, 캐비티, 누설유동

학 번: 2015-20739